Porous Particle Filtration

By

Tulsi Deshik Char

A thesis submitted to the

School of Graduate Studies

Rutgers, The State University of New Jersey

In partial fulfillment of the requirements

For the degree of

Master of Science

Graduate Program in Chemical and Biochemical Engineering

Written under the direction of

Nina Shapley

And approved by

_____

_____

_____

New Brunswick, New Jersey

May 2019

ABSTRACT OF THE THESIS

FILTRATION OF POROUS PARTICLES

by TULSI DESHIK CHAR

Thesis Director: Nina Shapley

Filtration is a widely used unit operation, particularly in catalyst manufacturing. The process is still largely empirical and requires extensive testing of the material in question and the equipment before predictions can be made about efficiency and performance. Even with extensive testing, subtle, often overlooked variations in input will result in an unexpected outcome, such as a failed filtration run. Our approach is to develop an experimental laboratory scale model that can relate key parameters to filtration behaviour. Experiments were performed on a benchtop Nutsche filter with constant applied pressure. Analysis of the filter cake and comparison with filtration performance provided insight in order to connect packing characteristics with material characteristics. Several porous catalyst materials were investigated. Darcy's law for constant pressure, which relates the filtrate volume with time, was applied to analyze the results and calculate the cake resistance.

Pure materials with various particle size distributions and median particle sizes were tested at several applied pressures. A mixture a 11% fine and 89% coarse porous material was also tested to examine the effect of fine particle addition on filtration behaviour. Even a small percentage of fines (11% of total solids) resulted in cake permeability and filtration time comparable to that of the pure fine particles.

The same particle size distributions were also tested in a continuous filtration set up and these results were compared to batch filtration runs with the Nutsche filter. It was observed that the effect of limited settling is favourable and could be a filter aid that does not chemically modify the cake.

ACKOWLEDGEMENT

I would like to thank my thesis advisor, Dr. Nina Shapley for her guidance and patience- her councel, insight and approachability made this project possible. I am grateful to Dr. Tewodros Asefa and Dr. Masanori Hara for their valuable critique on this project. I would like to thank Bill Boghard for his input on all presentations and during meetings. This project would not have been viable without the support of Dr. Ben Glasser and the Industrial members of the Catalyst Manufacturing Consortium. This project is also beholden to Tom English and Dave Mest of Evonik. I am grateful to Zainab Abd Al-Jaleel for teaching me the skill set I needed for this project and Malvern Labs for the use of their instrunments.

I would like to thank the administrative and teaching faculty in the Chemical and Biochemical Engineering department for being helpful and open to questions, when I needed answers. I would like to thank my friends for keeping me grounded throughout this project.

Most importantly, I am forever indebted and grateful to my parents, Deshik and Jyothi Char and my brother, Gautam Char. Any and all my achievements are possible only because of their emotional and financial support, their respect for education and desire that I be happy.

TABLE OF CONTENTS

Title		Page number
	ABSTRACT OF THE THESIS	ii
	ACKOWLEDGEMENT	iii
	LIST OF TABLES	vi
	LIST OF FIGURES	vii
I.	INTRODUCTION	1
i.	Modes of Filtration	1
ii.	Industrial Problems with Filtration	2
iii.	Significance of this study	3
		5
II.	THEORY	5
i.	Darcy's Law	7
ii.	Carman Kozeny Equation	8
iii.	Ergun Equation	
III.	MATERIALS AND METHODOLOGY	9
i.	Characterization of Powders	10
ii.	Particle Size Distribution	12
iii.	Zeta Potential	12
iv.	Batch Filtration Runs	13
v.	Cake Analysis	15
vi.	Continuous Filtration Runs	15
vii.	Optimization of Experimental conditions for Filtration Runs	16
viii.	Results with model material	18
ix.	Batch to Batch Variability	18
x.	Trends with the model material	19
IV.	RESULTS	20
i.	Particle Size Distribution	20
ii.	Microscope Images of Powders	21
iii.	Zetasizer Results	22
iv.	Compressibility of dry powder	23
v.	Permeability of dry powder	25
vi.	Carman Kozeny Equation	25
vii.	Ergun Equation	27
viii.	Batch Filtration at Rutgers for Pure Materials	28
ix.	Batch Filtration of Coarse and Fine Mixture	42
x.	Continuous Filtration of Porous Particles	45

V.	CONCLUSION	52
VI.	REFERENCES	53

LIST OF TABLES

Title		Page number
Table 1.	Zeta potential values for Catapal A, Fine Alumina and Zeolite Y	23
Table 2.	Bulk and Tapped Density values for Porous Particles from The FT4 and AutoTap.	24
Table 3.	Permeability of cake and Resistance of cake values for each pressure with 1 micron screen. The cake permeability is higher by an order of magnitude for 12 psi and for 25 psi and 35 psi the permeability and resistance are more consistent.	33
Table 4.	Fines/Coarse ratio for each layer in the Fine Catapal A cake at 12 psi, 25 psi and 35 psi.	37
Table 5.	Permeability and cake resistance values for Fine Alumina at two different pressures, 12 psi and 35 psi with 1 micron screen.	38
Table 6.	Permeability and cake resistance values for Fine Catapal A, Fine Alumina and Zeolite Y at 12psi with 1 micron screen.	41
Table 7.	Permeability of cake and Resistance of cake values for each material at 12 psi with 1 micron screen. Experimental values of Cake height and Time of Filtration are also depicted.	44
Table 8.	Cake resistance and Time of Filtration for 200mL for Continuous filtration runs conducted at 35 psi.	45
Table 9.	Fine Alumina Filtration results for cake resistance and time of filtration for 200mL at 12 psi 1 micron screen.	48
Table 10.	Fine Catapal A Filtration results for cake resistance and time of filtration for 200mL at 12 psi1 micron screen.	49
Table 11.	Fine Alumina Filtration results for cake resistance and time of filtration for 200mL at 35 psi1 micron screen.	50
Table 12.	Fine Catapal A Filtration results for cake resistance and time of filtration for 200mL at 12 psi1 micron screen.	51

Title		Page number
Figure 1.	A. Linear plot of t/V vs V in differential form. B. Linear plot of t/V vs V in integrated form	7
Figure 2.	A. Pictorial depiction of FT4 compressibility measurement by application of normal stress on the powder column. B. Pictorial depiction of FT4 permeability measurement under increasing normal stresses.	10
Figure 3.	Freeman Technology Rheometer.	11
Figure 4.	Benchtop Nutsche Filter with 4'' diameter and pressure gauge.	13
Figure 5.	Result of glass bead filtration. The cake has been built up over the screen and is sitting on the bottom platform of the filtration equipment.	16
Figure 6.	Particle Size Distribution of Zeolite Y, Fine Alumina and Fine Catapal A of powders in liquid (water).	21
Figure 7.	Microscope images at 50x magnification for A. Fine Catapal A, B. Fine Alumina and C. Zeolite Y in a dilute suspension in water.	22
Figure 8.	Bulk Density at different normal stresses for porous and non-porous particles. Data from the FT4. Normal Stress 0 – 12 psi	24
Figure 9.	Permeabilities at different normal stresses for porous and non-porous particles. Data from the FT4. Normal Stress 0 – 12 psi	26
Figure 10.	Permeability vs. Porosity plot for Zeolite Y, Fine Catapal A, Fine Alumina against the Carman Kozeny Model for κ/d2 vs ε with K=5 and S=6/diameter.	26
Figure 11.	Ergun equation with diameters of 27.8 μm, 6.4 μm and 1 μm plotted against Carman Kozeny equation.	27
Figure 12.	Permeability vs. Porosity plot for Zeolite Y, Fine Catapal A, Fine Alumina against the Carman Kozeny Model for κ/d2 vs ε with K=5 and S=6/diameter and the Ergun Equation for diameter 28.7μm.	28
Figure 13.	The particle size distribution for the porous catalyst material (Catapal A surrogate); analyzed by laser diffraction liquid module. D50= 65.0 μm.	28
Figure 14.	A. Plots of t/V vs. V for 900 mL slurry of 20% Catapal A surrogate and 1 micrometer screen mesh size within 25psi applied pressure drop B. integral plot for typical deviation from linearity	30

Figure 15.	A. Particle Size Distribution for the layers of the cake show that the average particle size increases as we go down to the base of the cake and is consistent for the last layers. B. Bulk Density measurement of the layers of the cake.	31
Figure 16.	Comparison of Coarse, Fine and Raw Catapal A Particle Size Distributions measured by Laser Diffraction. The sieved particles have a narrower distribution.	32
Figure 17.	Plots of t/V vs. V for 900 mL slurry of 10% Fine Catapal A surrogate and 1 micrometer screen mesh size within 12 psi, 25 psi and 35 psi applied pressure drop.	33
Figure 18.	Figure 18: Bulk Density Layer Analysis for Filter Cake of Fine Catapal A, filtered at 12 psi with a 1 micron screen.	34
Figure 19.	Particle Size Distribution Layer Analysis for Filter Cake of Fine Catapal A filtered at 12 psi with a 1 micron screen.	34
Figure 20.	Bulk Density Layer Analysis for Filter Cake of Fine Catapal A filtered at 25 psi with a 1 micron screen.	35
Figure 21.	Particle Size Distribution Layer Analysis for Filter Cake of Fine Catapal A, filtered at 25 psi with a 1 micron screen.	35
Figure 22.	Bulk Density Layer Analysis for Filter Cake of Fine Catapal A filtered at 35 psi with a 1 micron screen.	36
Figure 23.	Particle Size Distribution Layer Analysis for Filter Cake of Fine Catapal A, filtered at 35 psi with a 1 micron screen.	36
Figure 24.	Time/Volume vs Volume for Fine Alumina at 12 psi and 35 psi.	38
Figure 25.	Bulk Density Layer Analysis for Filter Cake of Fine Alumina, filtered at 35 psi with a 1 micron screen.	39
Figure 26.	Particle Size Distribution Layer Analysis for Filter Cake of Fine Alumina, filtered at 35 psi with a 1 micron screen.	39
Figure 27.	Normalized Bulk Density comparison between Fine Catapal A and Fine Alumina for filter cakes from 35 psi runs with a 1 micron screen.	40
Figure 28.	Time/Volume vs Volume for Fine Catapal A, Fine Alumina and Zeolite Y at 12 psi .	41
Figure 29.	Particle Size Distribution Layer Analysis for Filter Cake of Zeolite Y filtered at 12 psi with a 1 micron screen.	42
Figure 30.	Comparison of Sieved Catapal A, Fine Alumina and 11% Fine Alumina and 89% Coarse Alumina.	43

Figure 31.	Plots of t/V vs. V for 900 mL slurry of 10% Catapal A, 10% Fine Alumina and 1.1% FA and 8.9% CA and 1 micrometer screen mesh size within 12 psi, 25 psi and 35 psi applied pressure drop.	44
Figure 32.	Filtration curves of t/v vs V for continuous filtration at 35 psi.	46
Figure 33.	Figure: Particle Size Distribution of slurries sampled from the reactor that feeds into filter housing for runs with Fine Alumina, Fine Catapal , Coarse Catapal A, Fine Alumina and Fine Catapal A mixture..	47
Figure 34.	Fine Alumina Filtration run curves at 12 psi.	48
Figure 35.	Fine Catapal A Filtration run curves at 12 psi.	49
Figure 36.	Fine Alumina Filtration run curves at 35 psi.	50
Figure 37.	Fine Catapal A Filtration run curves at 35 psi.	51

I. INTRODUCTION

i. Modes of Filtration

Filtration is a solid-fluid separation process that is performed by use of a filter medium which allows the passage of the fluid and partially restricts that passage of the solid, depending on the characteristics of the medium and the two phases. It also depends on the mechanism by which the filtration is conducted.

The separation is incomplete, for example, moisture on solids and turbidity in liquids. If solid is the component of interest in the solid liquid separation process, the solids will also have to be processed by washing, deliquoring and drying. Washing will remove liquids impurities in interparticle pores, deliquoring is the mechanical separation of liquid and drying is the thermal removal of liquid.

Filtration can be classified by: (i) Location of particle retention on the filter medium, (ii) Mechanism of driving force application, (iii) Mode of operation and application.

There are four idealized models of filtrations:

a) Cake Filtration: The most common form of filtration, where the particles are deposited upstream and lie on top of the filter. When the first homogeneous layer is formed, the subsequent filtration does not take place due to the filter but due to the layer of particles.

b) Blocking Filtration: This form of filtration takes place when the pores are blocked by incoming particles, with constant incoming flow rate, this results in an exponential pressure drop[1]

c) Deep Bed Filtration: Particles are caught deep in the filter retained by the screening effect, especially bigger particles.

d) Cross Flow Filtration: Solids are retained on the filter, tangential flow of fluid prevents the building of the cake. At steady state, equilibrium is reached between the flow of liquid through the filter and the tangential flow across the filter.[2, 3]

ii. Industrial Problems with Filtration

Although filtration is an old and widely used process, even now the process is largely empirical, where it is difficult to predict the actual rate of filter cake formation and the required pressure drop or flow rate.

Given that filtration is such an essential process in many industries, the problem of batch to batch variation must be acknowledged and addressed. One reason for this could be the presence of fines that may dominate the behavior of filtration. fine particles play an important role in many industries, such as ceramics, minerals, pigments, cosmetics, electronics, and pharmaceutical industries. Fines have the potential to increase the difficulty of filtration by blocking the pores of the cake. A difficult filtration run translates into a long filtration run.[4] This is undesirable in industrial applications.

One option to prevent this is a possible pretreatment step.[5] In the experimental method detailed in this document, sieving is used to modify the particle size distribution to increase cake permeability. Popular approaches for helping to increase cake permeability include flocculation, back-pulsing[6], embedded structural supports, and surface patterning or treatment of the filter membrane or cloth. Flocculation is used frequently to aid cake filtration - The flocculant is typically a polymer, often with opposite charge

attraction to the particles, that needs to be burned off during subsequent processing steps. [7, 8]

Other commonly faced problems in industrial filtration are:

a) Low flow rates and very high pressure drops, arising from too close packing of the particles in the filter cake.

b) Insufficient washing of the resulting filter cake to clean it from electrolytes and if the cake is not washed adequately, this can lead to potential catalyst inactivation. In addition, one would like to minimize the water used for washing as often this water requires subsequent treatment.[9, 10]

c) Low particle capture arising from excessive dilution of the suspension.

d) Change in cake formation rates, pressure drops and flow rates over time.[11-13]

iii. Significance of this study

The powders used in this study are catalysts and catalyst precursors used in industrial processes. Filtration is a common process during catalyst manufacturing and re-use. The inability to efficiently filter the catalysts can lead to inactivation due to electrolytes and inefficient recycling due to poor particle capture.

The unique contributions of this thesis are the focus on the cake filtration behavior of porous particles and the analysis of the microstructure of the resulting cakes. Catalyst particles are generally porous. Therefore, previous literature results obtained from nonporous model particles, such as glass beads , likely do not fully capture the filtration behavior of porous particles, where the intra-particle pores may play a role in flow through

the porous medium. Moreover, only a few previous studies have analyzed filter cake microstructure in selected systems[14, 15]. This study aims to enhance understanding of filtration behavior by capturing the average particle size distribution and bulk density of the filter cake as well as the variation of these properties with height in the cake. By characterizing the powders and relating that to filtration behavior it is possible to link poor filterability with material characteristics. Fines significantly control the behaviour of filtration.[16, 17] Once this correlation is established is possible to modify poorly filtered materials to get better filtration behavior.

Goals:

a) Using the benchtop Nutsche filter to run constant pressure filtration experiments with various catalyst materials and measuring cake resistance and permeability
b) Characterizing the catalyst materials and noting the dependence of ease of filtration on these measured characteristics
c) Analyzing bulk density and particle size distribution in each layer of the filter cake
d) Running filtration experiments in a continuous setting and comparing the cake resistances to those measured in a batch system.

II. THEORY

i. Darcy's Law

Darcy's law states that the pressure drop of a liquid flowing through a porous bed is proportional to the following factors:[3, 18]

a) Flux through the porous medium henceforth symbolized as $(\frac{\dot{V}}{A})$

b) The thickness of the cake that has been built up henceforth symbolized as H

c) The viscosity of the liquid flowing through the porous bed henceforth symbolized as η

d) The specific filter resistance of the cake henceforth symbolized as α

OR inversely proportional to the specific filter permeability henceforth symbolized as $\frac{1}{K}$

As a result, we get:

$$\Delta P_1 = \eta\ \alpha\ \left(\frac{\dot{V}}{A}\right) H \quad (1)$$

Rearranging the terms, the equation takes on a familiar form,

$$Q = \left(\frac{\dot{V}}{A}\right) = \frac{\kappa}{H\ \eta}\ \Delta P \quad (2)$$

This is analogous to Fick's law of diffusion, Fourier's law of heat conduction and Ohm's law for heat conductivity.[2]

ΔP_1 the pressure drop across the cake height, consider ΔP_2 the pressure drop across the filter medium. The cake resistance is responsible for significantly higher pressure drop.

$$\Delta P_2 = \beta\eta\left(\frac{\dot{V}}{A}\right) \quad (3)$$

The total pressure drop across the filter and the cake is

$$\Delta P = \Delta P_1 + \Delta P_2 \quad (4)$$

Cake filtration can either be constant pressure or constant flowrate filtration. The benchtop Nutsche filter is set-up to allow compressed air to apply a constant pressure on its contents ($\Delta P = \Delta P_1 + \Delta P_2$=Constant)

$$\Delta P = \eta . \alpha . \left(\frac{\dot{V}}{A}\right) . H + \beta . \eta . \left(\frac{\dot{V}}{A}\right) \quad (5)$$

K_H is a factor that describes the influence of cake porosity and concentration.

$$\Delta P = \eta . \alpha . \left(\frac{dV}{dt}\right) . \left(\frac{V}{A^2}\right) . K_H + \beta . \eta . \left(\frac{dV}{dt}\right) . \frac{1}{A} \quad (5)$$

On Integration with respect to differential volume

$$t = X.V^2 + Y.V \quad (6)$$

$$X = \frac{K_H \eta \alpha}{2 \Delta P A^2} \qquad Y = \frac{\beta \eta}{\Delta P A} \quad (7)$$

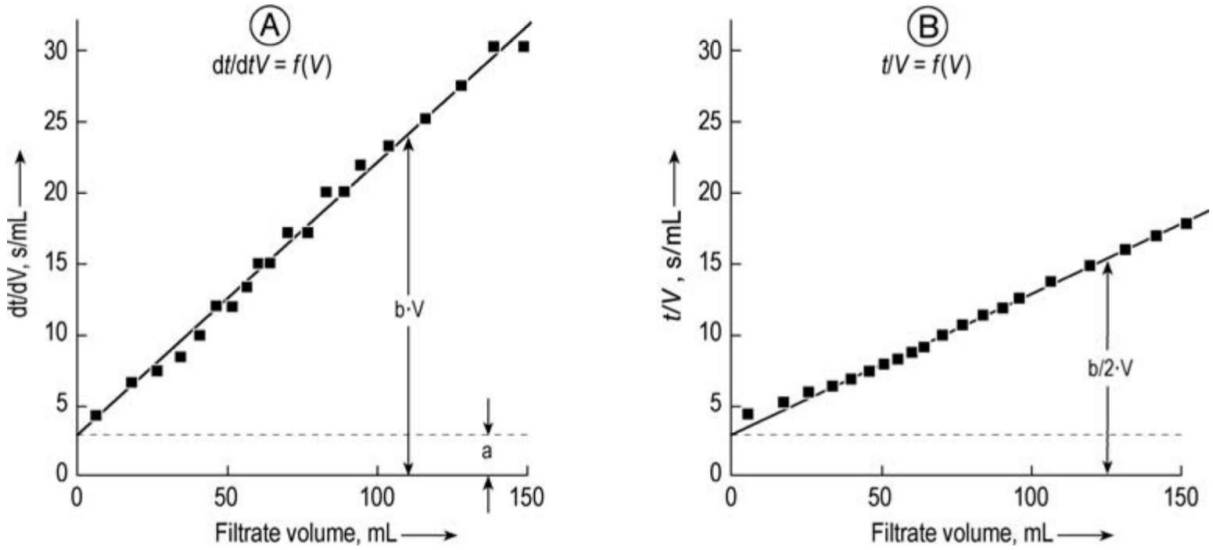

Figure 1: A. Linear plot of t/V vs V in differential form B. Linear plot of t/V vs V in integrated form[2]

The plot in Figure B. is used heavily in the experiments described in this document. It is easy to plug in experimental values of measured flowrate and get a the permeability of the filter cake. [19]

ii. Carman Kozeny Equation

The Carmen Kozeny equation relates powder bed permeability to porosity. The porosity is defined by void fraction.

$$\varepsilon = 1 - \frac{\rho_{bulk}}{\rho_{true}} \quad (8)$$

The permeability can be related to void fraction as follows.

$$K = \frac{1}{KS^2} \frac{e^3}{(1-e)^2} \quad (9) \quad [2, 20, 21]$$

With K representing permeability, K is known as the Kozeny constant (with a typical value of 5) and S is the specific surface area (with a value of 6/diameter for spherical particles).

iii. Ergun Equation

The Ergun equation is a modified Carman Kozeny equation. It accounts for tortuosity of the pores of the porous bed. It also expresses pressure drop as a combination of two contributions, a viscous effect and an inertial effect.

$$\frac{d_p^2}{\kappa} = \frac{(1-\varepsilon)^2}{e^3}\left(150 + 1.75\,\frac{\rho u_s d_p}{(1-\varepsilon)\mu}\right) \quad (10)$$ [20, 22]

III. Materials and Methodology

The materials used in this study are Catapal A supplied by Sasol, Fine Alumina supplied by Albermarle and Zeolite Y supplied by Zeolyst International. Previous experiments were performed on Glass beads purchased from the Mo Sci Corporation.

i. Characterization of Powders

Compressibility and Permeability of Dry Powder: The Freeman FT4 powder is used in studies of powder cohesion, where the permeability is an indicator of the cohesiveness of the particles.[23] The flow-rate pressure drop curve can then be applied to scale-up calculations Compressibility is measured by applying increasing levels of compressive force with a piston to a powder and measuring the change in volume as a function of the applied load. The Freeman FT4 rheometer is used to measure the permeability of a uniform bed of particles to air flow as a function of applied normal stress. Permeability is a measure of the powder's resistance to air flow. The applied normal stress is similar to the compression of the filter cake by the fluid flow pressure drop and by the weight of the portion of the filter cake above. The relative difference in air pressure between the bottom and the top of the powder column is a function of the powder's permeability. [23, 24]

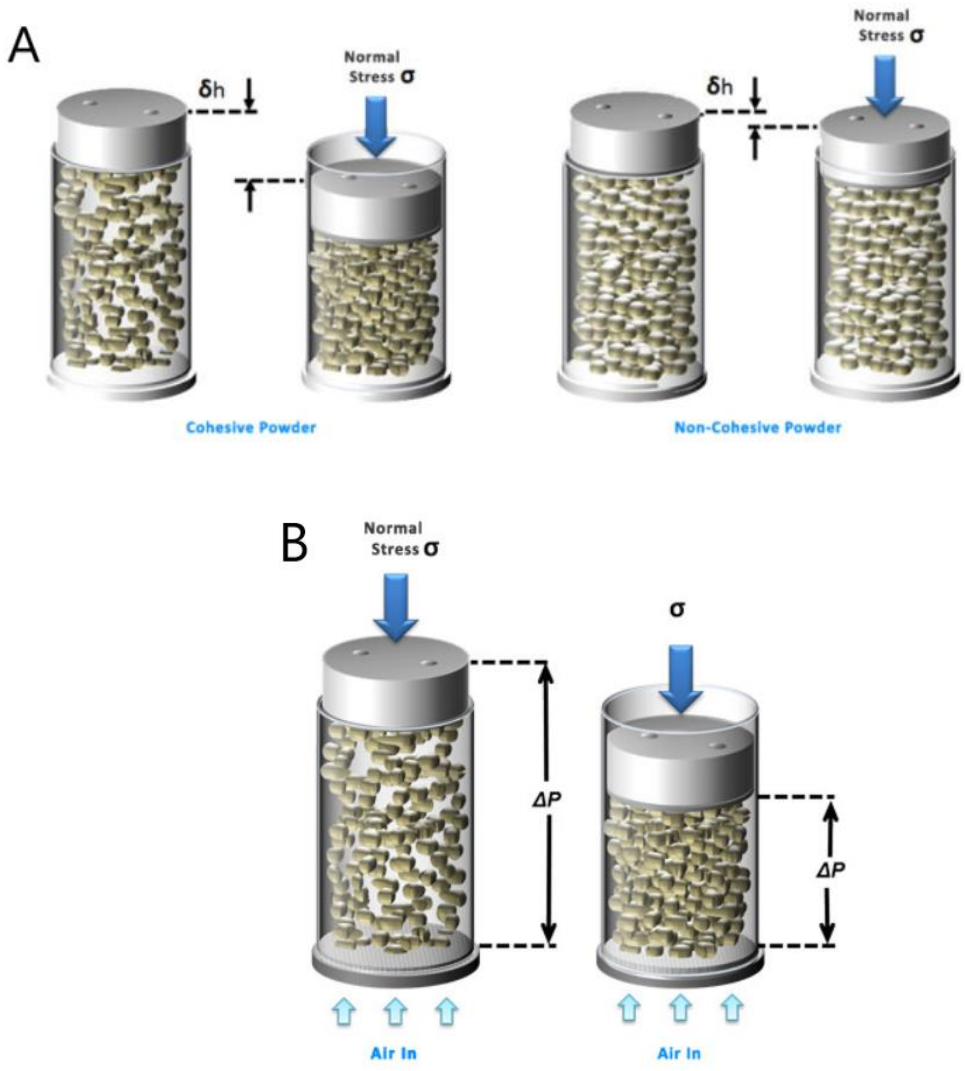

Figure 2: A. Pictorial depiction of FT4 compressibility measurement by application of normal stress on the powder column. B. Pictorial depiction of FT4 permeability measurement under increasing normal stresses.[25, 26]

$$Bulk\ Density = \frac{Mass\ of\ powder\ in\ column}{Volume\ after\ compression}\ g/ml \quad (11)$$

$$Compressibilty\ Index = \frac{Density\ after\ compression}{Original\ Bulk\ Density} \quad (12)$$

$$Permeability = \frac{q\mu L}{\Delta P} \qquad (13)$$

q = flowrate of air through powder column; μ = viscosity of air;

L = length of powder column;

ΔP = Pressure drop across powder column

The standard methodologies for the FT4 equipment can be modified and can be accessed under user defined methodologies

Figure 3: Freeman Technology Rheometer

The FT4 has a normal stress range of 3 Kpa - 85 Kpa. Programming the FT4 to gradually apply 85 Kpa of normal stress we can test compressibility and air permeability at conditions close to what the filter operates on i.e. 12 psi.

Equipment:

The FT4 powder Rheometer from Freeman Technology is used to measure the bulk properties of the dry powders.

ii. Particle Size Distribution:

Particle size distribution analyses the relative amount, by volume, of different sizes of particles.

Equipment:

Beckman Coulter LS 13 320 Laser Diffraction Spectrometer, liquid module was used for particle size measurement of the powders.

General Procedure:

The powders were diluted in water and sonicated. Samples are not allowed to settle before loading into the equipment. The spectrometer can also sonicate the sample while loading and measuring. The results give us particle size distribution, size mean and median.

iii. Zeta-potential

The zeta-potential of the powders suspended in deionized water was measured. The zeta potential is proportional to the surface charge density and indicates the degree of electrostatic repulsion among the particles.

Equipment:

The zeta-potential of the powders were measured by Malvern Instrument's Zetasizer Ultra.

iv. Batch Filtration Runs

Equipment:

The benchtop Nutsche filter [27] from Pope Scientific is the equipment on which the filtration runs, described in this document, are conducted. It is a 1 litre vessel, oriented vertically, as pictured below.

Figure 4: Bechtop Nutsche Filter with 4'' diameter and pressure gauge

It consists of three main parts, the lid, connected to the regulator for compressed air and the gauge that reads in pounds per square inch, the filter body that is a vertical cylinder like vessel with sight glasses. The filter has four sight glasses and the inside is marked with a height scale to monitor the filtration inside the vessel.

The filter is mounted over the platform, and this has a pipe outlet that can be directed to a beaker to collect the outlet flow i.e. filtrate. Each individual part is connected to the next

by a clamp and the apparatus can be sealed by tightening the clamp. Each fastening point of the filter is equipped with an ‘O’ ring and gasket to prevent leakages. The clamps are tightened considerably, to prevent leakage, with the help of a wrench.

Once everything is fastened, compressed air is regulated through the filter to drive the filtration process.

The setup also includes a weighing scale connected to a computer. A beaker is placed on the scale, where the filtrate is collected. Software records the rate of filtrate collection.

The filtration runs carried out with the benchtop Nutsche filter are batch, pressure driven cake filtration runs. A general procedure is given below.

a) A predetermined weight of powder is carefully scooped into a 1 litre beaker. Care must be taken to ensure that the fines present don’t separate. This is especially important for dusty powders where the fines can aerolize and distort the particle size distribution of the slurry.
b) The slurrying liquid is poured gently into the same beaker until the slurry reaches a required concentration,
c) The mixture is pre-mixed gently with a glass rod. The slurry is then prepared over a stir bar magnetic mixer for 30 minutes at 600 rpm.
d) A clean and prepped screen is placed in the filter and the filtration apparatus is assembled. The baseline resistance of the filter is measured with deionized water at atmospheric pressure.
e) Once the mixture has been adequately mixed to ensure no pockets of air or powder, the slurry is gently poured into the filter. Care is taken to ensure that the slurry is poured straight down to try and maintain radial symmetry.

f) The lid s fastened. The time of manual fastening contributes to a non zero waiting time of approximately two minutes. The optimization of waiting time has been detailed later in this document.

g) Air flow is regulated to exert a predetermined pressure that can be monitored by the pressure gauge.

h) Filtrate passes through the media into the beaker.

i) The rate of filtrate collection by weight is measured until no water can be seen over the cake. This can be observed from through the sight glasses in the filter.

j) The cake is carefully removed for analysis.

v. Cake Analysis

a) Samples of known volume are carved out of the cake

b) Layers are cut along the height of the known volume to get 4-6 layers at different heights from the top of the cake to the bottom.

c) Each layer is dried and measured to get the bulk density

d) Each layer is then sonicated in water and the particle size distribution is measured.

vi. Continuous Filtration Runs

Equipment:

Filtration runs were conducted in a continuous filter set up. It consists of a continuous stirred tank that pumps slurry to the filter housing under pressure. The filter was set up with a 1 micron screen for the experiments.

a) The slurry is prepared by the same procedure as for Batch Filtration and is poured gently into the reactor.

b) The agitator stirs at the rate of about 1000 rpm to prevent settling.

c) The baseline resistance of the filter is measured with water at 5 psi.

d) The slurry is pumped to the filter housing under pressure where it filters through the screen and builds up cake.

e) The rate of filtrate collection by weight is measured.[28]

vii. Optimization of Experimental conditions for Filtration Runs

The experimental conditions were optimized by carrying out various experiments with a model material. The model material selected was glass beads. Monodisperse glass beads are an ideal choice as a model material because they are non-porous and had a narrow particle size distribution.

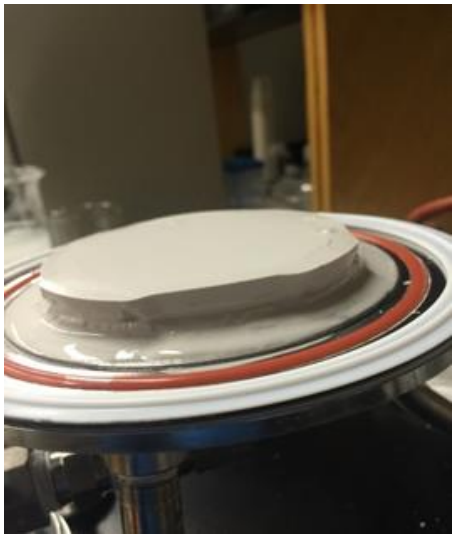

Figure 5: Result of glass bead filtration. The cake has been built up over the screen and is sitting on the bottom platform of the filtration equipment.

a) Slurry Volume:

The glass bead (model material) experimental runs were conducted at 500ml, 700mL and 900mL slurry volume. The 500mL slurry volume experiments resulted in more permeable filter cakes, compared to 700mL to 900mL slurries at 20 wt%, suggesting that the 500mL slurry volume does not have sufficient critical mass of particles for the bulk measurement. It is also much easier to analyze a cake that is taller as well as analyze each layer.

b) Screen Mesh Size

Screens with two different mesh sizes (1 and 5 micrometers) were used as the filter media., The 1 micrometer mesh screen shows a decrease in permeability with an increase in pressure for lower volumes, but an increase in permeability with an increase in pressure for higher volumes.

Conversely, the 5 micrometer mesh screen shows an opposite trend with pressure, probably because of the loss of fines during the beginning of the filtration before the cake builds. To get an appropriate number of data points and retain fines to study in cake analysis, it is better to use a 1 micron screen.

c) Operating Pressure Range:

The Benchtop Nutsche filter can pressurize up to 48 psi, consequently this value defines the pressure ranges the experiments were conducted in. Experiments conducted at the higher end of the pressure range have resulted in cracked cakes and failed filtration runs. Industry members associated with catalyst filtration were consulted on the project and they

recommended a pressure range of approximately 2-4 bar (~30-60 psi) Most of the experiments are conducted in the pressure range of 12 psi - 35 psi, which overlaps with the desired range..

d) Waiting Time:

Waiting time is the name assigned to the time assigned between pouring the slurry in and letting the pressure reach a certain pressure. It is a non-zero component because the fastening of the lid and regulating of compressed air to reach the pressure can take anywhere from 90 - 180 seconds. Experiments were conducted at varying waiting times. The results showed that at higher waiting times, the permeability change was small, but the time of filtration increased. An increased waiting time allows for settling. This isn't a very common practice in industrial filtration of catalysts. Consequent experiments were carried out with the minimum possible waiting time.

viii. Results with model material

The model material is monodispersed non porous glass beads. Multiple batches were ordered from the Mo-Sci Corporation. The two sizes of glass beads in the model material runs are mean diameter 8 μm and 30 μm, More focus is placed on the 8μm glass beads.

ix. Batch to Batch Variability

One of the goals of this project is to address the problem of batch to batch variability in different filtration runs experienced during industrial filtration. The batches of glass beads bought from Mo-Sci inadvertently posed the same problem. Different batches had different filtration behavior despite having the same mean size (8μm).

Compared to the first batch of glass beads, the second batch of glass beads filtered very differently. The cake for the second batch of glass beads was more prone to retaining water and the run was more likely to fail.

Examining the particle size distribution curves for both batches, it can be seen that the second batch of glass beads has a higher percentage of fines. It may be concluded that fines distribution is the dominating factor that can control filtration

x. Trends with the model material

Results with the model material showed a slight trend of increased permeabilities with an increase in applied pressure but resistance stayed the same. Raising the applied pressure from 12 to 35 psi through the various steps of filtration experiments didn't significantly affect the permeabilities and intercept resistances.

IV. RESULTS

i. Particle Size Distribution

The particle size distribution for each slurry was sampled before running the filtration experiment. The first series of experiments were run with Catapal A, However the particles were too large to run in our benchtop Nutsche filter and had to be sieved by a 53 micron mesh. The resulting fractions of Raw Catapal A are Fine Catapal A (<53 µm) and Coarse Catapal A (>53 µm).

Raw Catapal A has a broad particle size, it goes up to 200 µm. This broad distribution and high particle size disparity makes the material very difficult to handle the powder. The heavier particles settle easily making it difficult to get an accurate reading in a batch filter. Sieving Raw Catapal A allows for easier handling. However Fine Catapal A still settles, this settling is significant and might distort the results.

Fine Alumina has a much smaller median size and a much narrower particle Size distribution as can be seen in *Figure 6* below. The smaller particles are easier to slurry. The results can be trusted to not significantly have the additional aid of settling during filtration.

Zeolite Y has a much smaller d50 and a very narrow distribution. The particles are easy to slurry and don't settle.

The d50 of Fine Catapal A is 28.7 µm, Fine Alumina is 6.4 µm and Zeolite Y 1 µm.

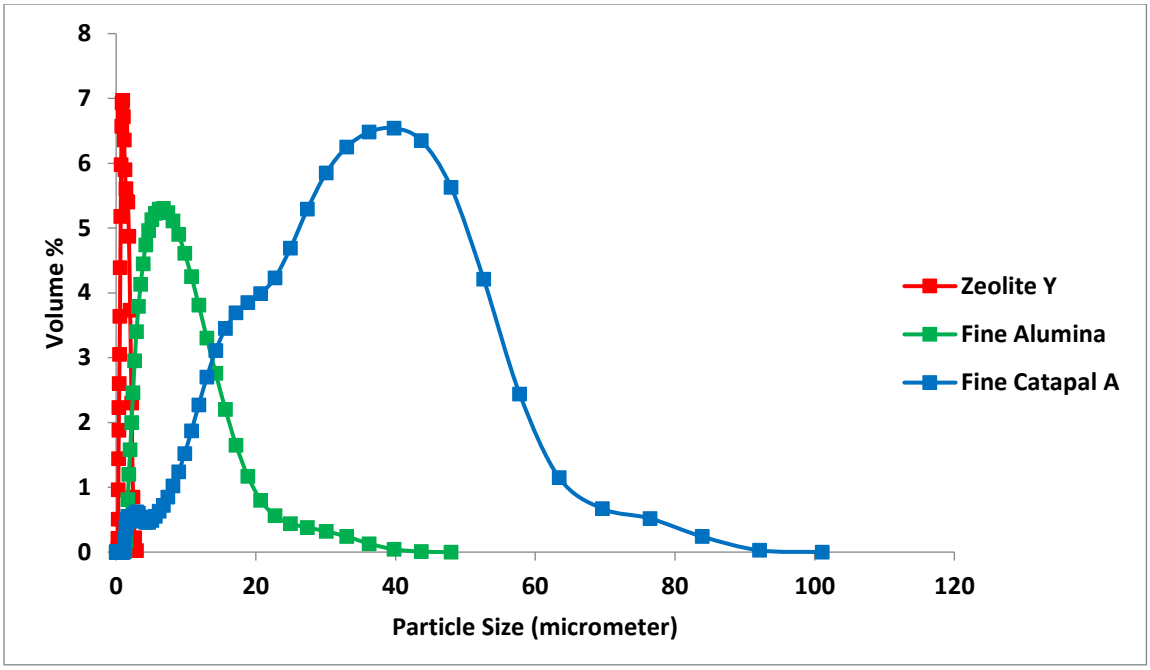

Figure 6: Particle size distribution of Zeolite Y, Fine Alumina and Fine Catapal A of powders in liquid (water)

ii. Microscope Images of Powders

Microscope Images were taken at 10x, 40x and 50x magnification. Microscope Images at 50x magnification are given below. The microscope images reveal that the particles are not spherical. The differences in sizes can also be seen visually. The images of the particles are taken in a dilute suspension

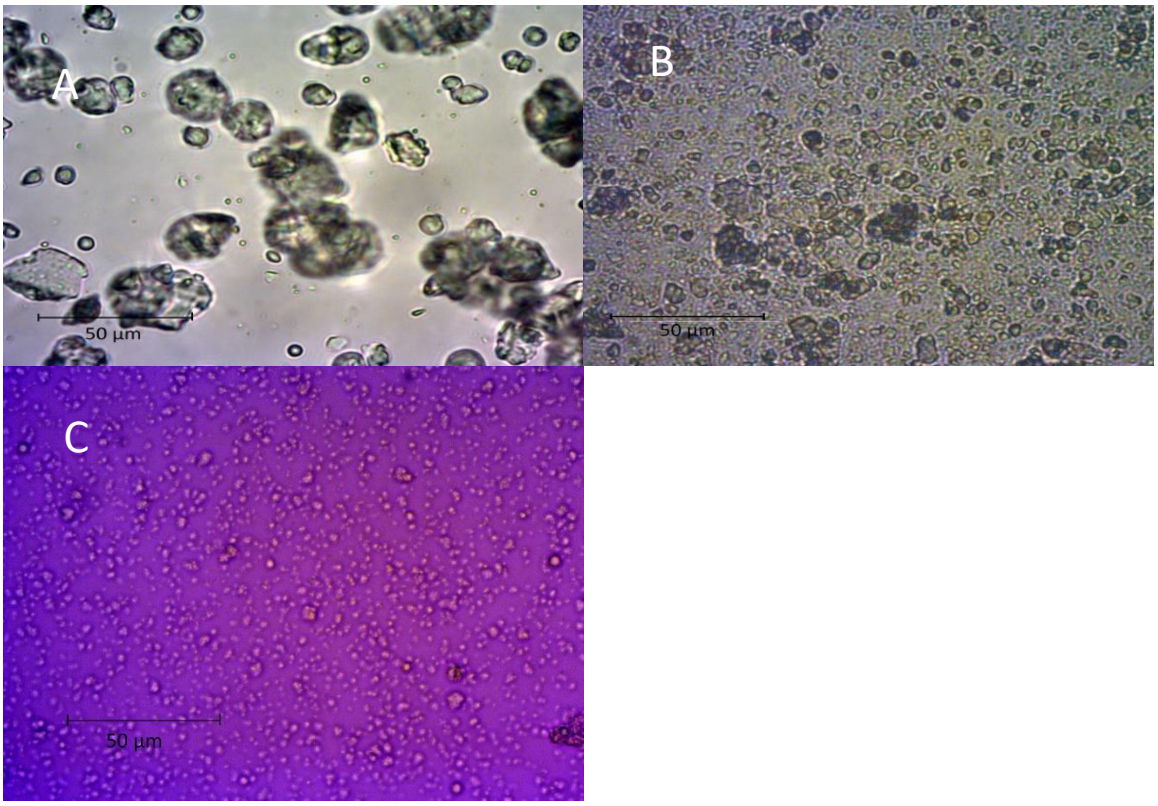

Figure 7: Microscope images at 50x magnification for A. Fine Catapal A, B. Fine Alumina and C. Zeolite Y in a dilute suspension in water.

iii. Zetasizer Results

Zetasizer measurements were taken. Raw Catapal A has a positive zeta potential of about 25mV – 30mV and Fine Alumina has a lower zeta potential at 15mV. Catapal A is on the verge of being a stable dispersion (the limit being 30mV). Fine Alumina is more unstable. Catapal A is more stable but the large particles settle out of the dispersion. Zeolite Y is stable at -40mV

Material	**ZetaPotential (mV)**
Raw Catapal A	26.9
Fine Catapal A	27.8±1.4
Coarse Catapal A	30.5
Fine Alumina	15.3±1.6
Zeolite Y	-40.0±0.8

Table 1: Zeta potential values for Catapal A, Fine Alumina and Zeolite Y

iv. Compressibility of dry powder:

The Freeman Technology Rheometer can be programmed to apply normal stresses up to 85 kpa (12 psi) to a conditioned (to ensure uniformity) powder bed. The high stresses are applied by a vented piston (to allow escape of trapped air) in the powder bed.

Figure 8 shows the trend of Bulk Density with Stress Applied for each batch of Glass Beads and the porous materials - Catapal A (Raw and Fine), Zeolite Y, Fine Alumina.

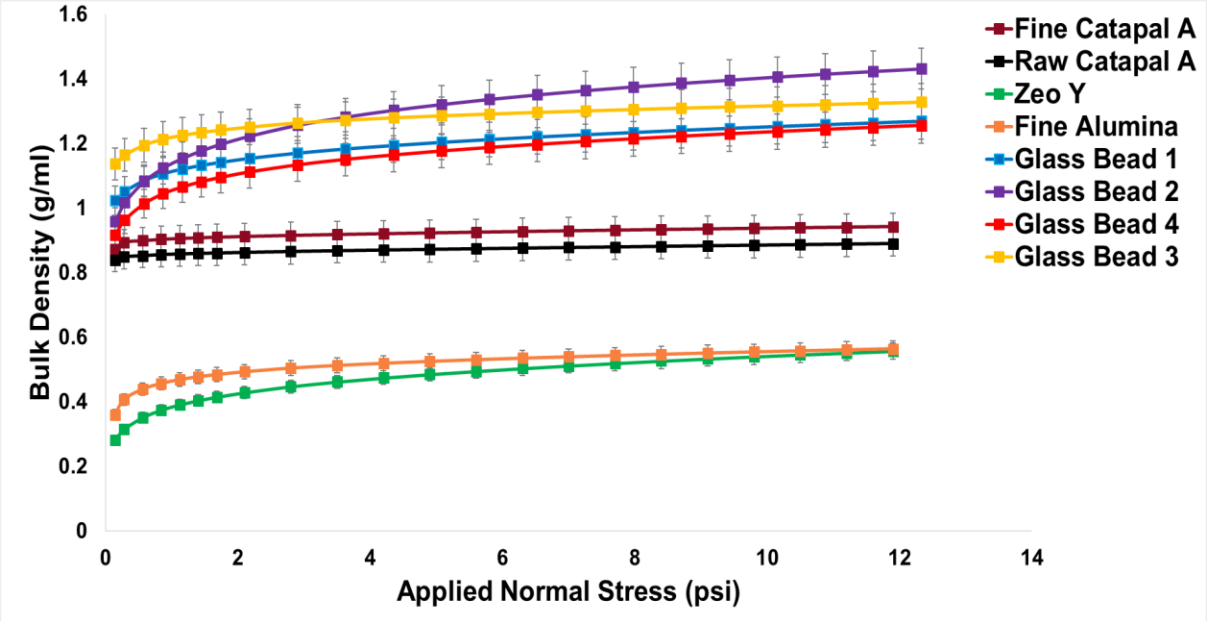

Figure 8:Bulk Density at different normal stresses for porous and non-porous particles. Data from the FT4. Normal Stress 0 – 12 psi

Focusing on porous particles specifically, the values of densities at very high pressures are given below in Table 2.

	Bulk Density	**Tapped Density**	**Final Bulk Density @ 85kPa**	**% Compressibility @ 85kPa**
Raw Catapal A	0.83 g/ml	0.97 g/ml	0.89 g/ml	6.90%
Fine Catapal A	0.86 g/ml	1.04 g/ml	0.94 g/ml	8.95%
Fine Alumina	0.29 g/ml	0.39 g/ml	0.56 g/ml	48.20%
Zeolite Y	0.22 g/ml	0.335 g/ml	0.56 g/ml	61.22%

Table 2: Bulk and Tapped Density values for Porous Particles from The FT4 and AutoTap for Tap Density.

Glass beads have a consistently higher bulk density, even under much higher pressures at 12 psi. Amongst the porous particles measured Zeolite Y is the least dense, followed by fine alumina. The low density of these particles are a result of their porosity and interparticle forces that might possibly dominate at that particles size range.

It is important to note that Catapal A is barely compressible in dry powder state. Fine Alumina and Zeolite Y are highly compressible in dry powder state, Zeolite compresses up to 61.22%.

Permeability of dry powder:

Figure 9 shows the permeability measurements taken by the Freeman rheometer for the materials. The different batches of glass beads show similar trends of permeability but different values. Only changes in orders of magnitude are considered significant. We can see a significant difference between Raw Catapal A and Zeolite Y.

Raw and Fine Catapal A do not show a smart decline in permeability due to pressure. Zeolite Y shows a sharp decline in permeability up to 2 psi pressure.

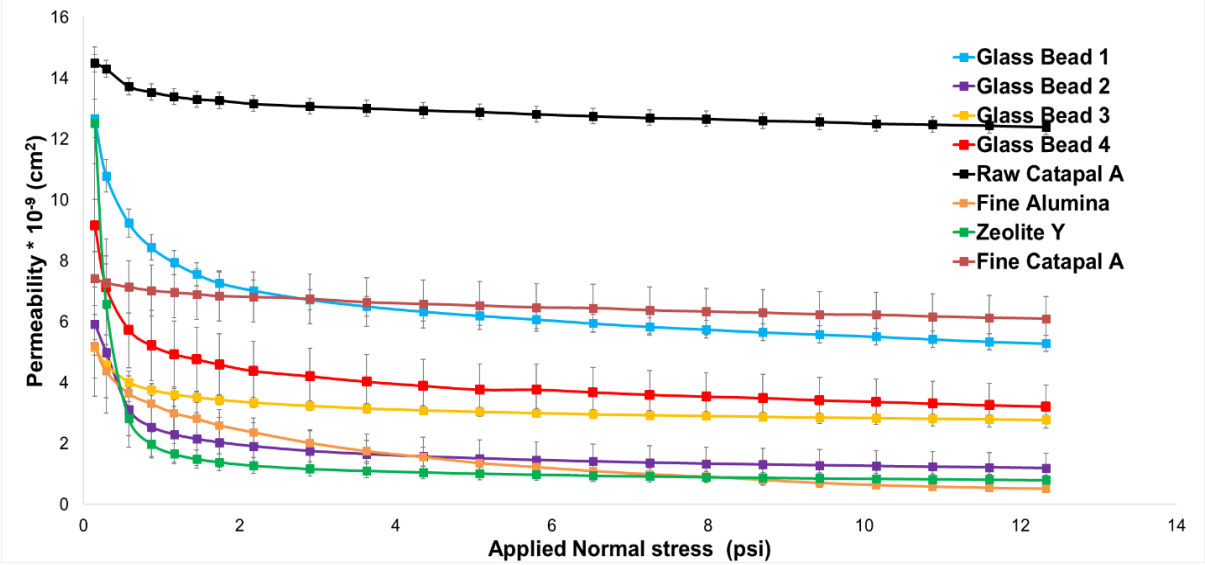

Figure 9: Permeabilities at different normal stresses for porous and non-porous particles. Data from the FT4. Normal Stress 0 – 12 psi

v. Carman Kozeny Equation

The model is plotted in the graph in Figure: with K=5 and S=6/diameter.

$$K=\frac{1}{KS^2}\ \frac{e^3}{(1-e)^2}$$

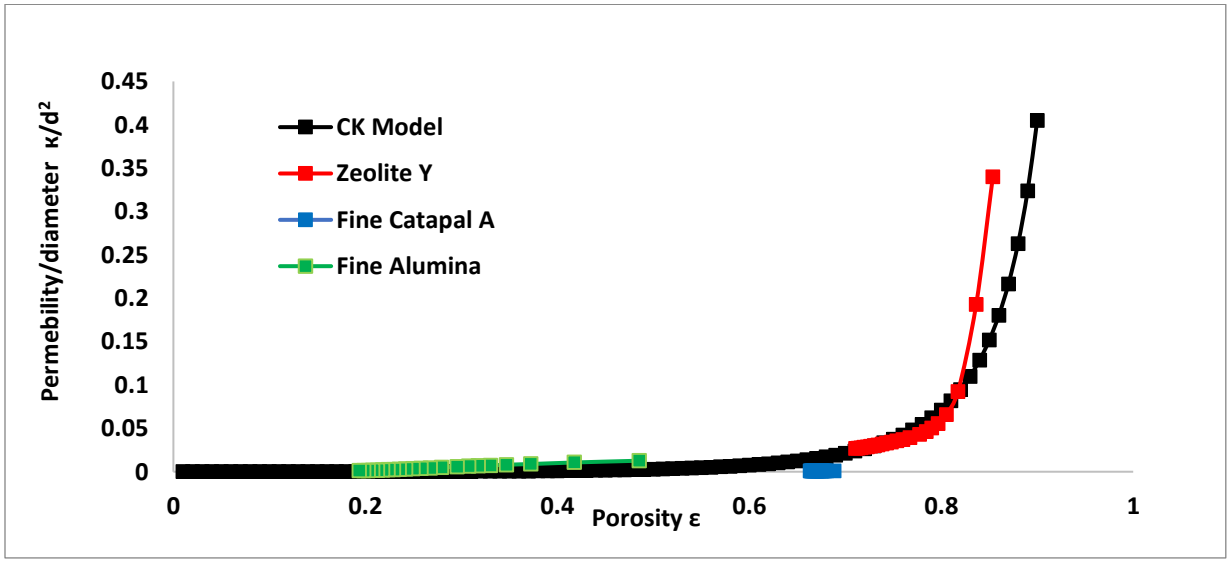

Figure 10: Permeability vs. Porosity plot for Zeolite Y, Fine Catapal A, Fine Alumina against the Carman Kozeny Model for κ/d^2 vs ε with K=5 and S=6/diameter

vi. Ergun Equation

$$\frac{d_p^2}{\kappa} = \frac{(1-\varepsilon)^2}{e^3}\left(150 + 1.75\frac{\rho u_s d_p}{(1-\varepsilon)\mu}\right)$$

Where ρ is the density of the fluid (air at 20°C) and μ is the viscosity of fluid (air at 20°C). The Carman Kozeny model is plotted with the Ergun model in Figure below. At lower permeabilities the inertial contribution is very negligible, and the points overlap. In Figure the graph with the axis zoomed in to show the differences. It can also be seen that the Ergun models for various diameters overlap completely i.e. a very negligible change.

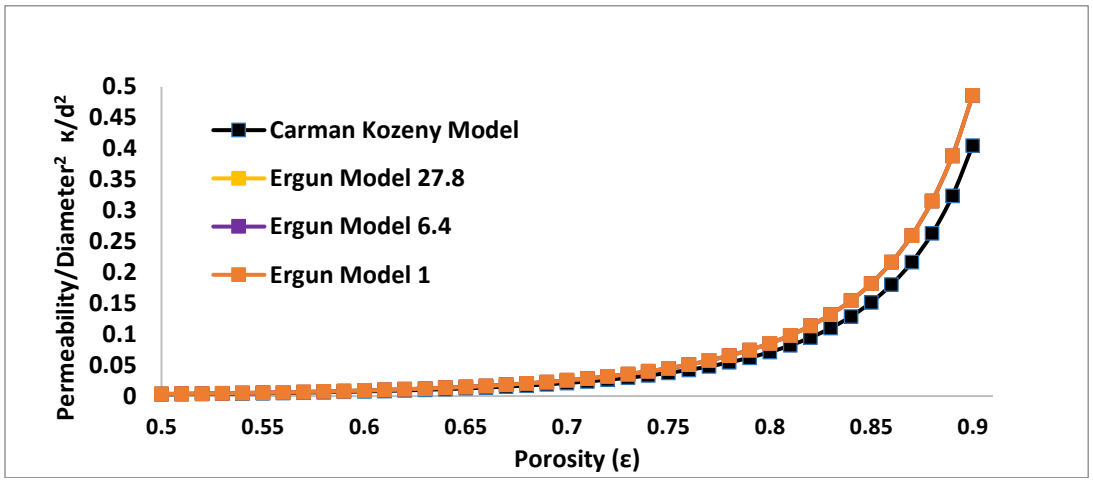

Figure 11: Ergun equation with diameters of 27.8 μm, 6.4 μm and 1 μm plotted against Carman Kozeny equation.

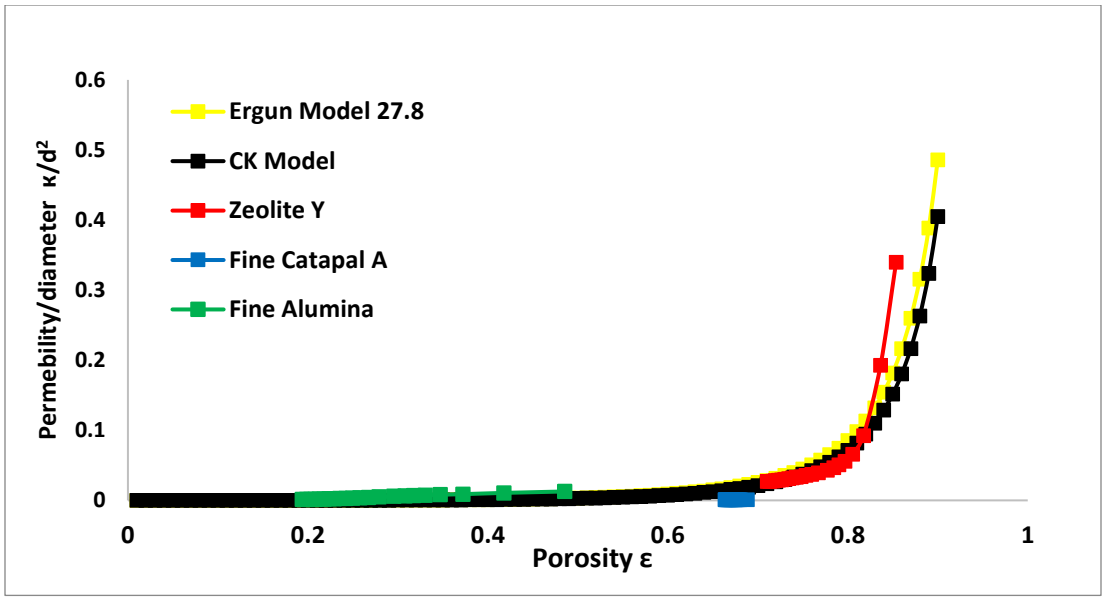

Figure 12: Permeability vs. Porosity plot for Zeolite Y, Fine Catapal A, Fine Alumina against the Carman Kozeny Model for κ/d^2 vs ε with K=5 and S=6/diameter and the Ergun Equation for diameter 28.7µm

vii. Batch Filtration at Rutgers for Pure Materials

Initial Experimental Runs were conducted with 20% w/w slurry (same as glass beads) and 25psi pressure with Raw Catapal A. The screen was a 1 micron screen.

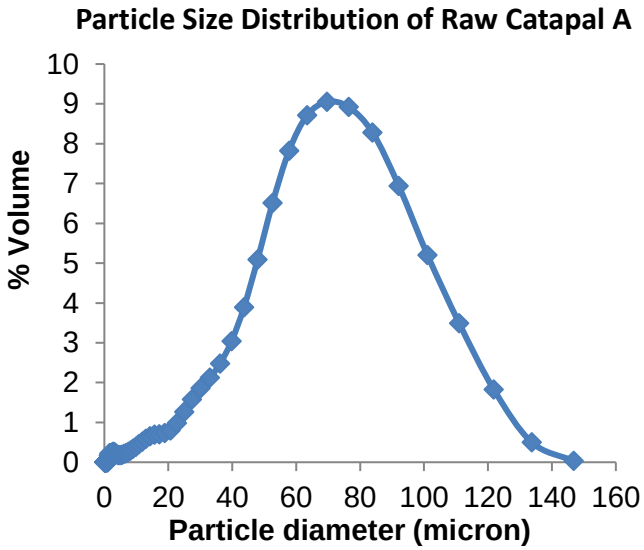

Figure 13: The particle size distribution for the porous catalyst material (Catapal A surrogate); analyzed by laser diffraction liquid module. D50= 65.0 µm

Comparing our experimental curves (20% Catapal A, 25psi, I micron screen – Figure 14 A) to the examples found in *Ullmann's Encyclopaedia of Industrial Chemistry[3]* (Figure 14 B), It can be compared to F in figure 14 B which indicates that possible block of media pores by fines and/or significant settling.

Plotting t/V vs V to measure permeability we get an average $\kappa = 1 \times 10^{-11}$ cm^2.

Analysis of the cake layers also show that settling is significant. Figure 15(a) shows that the particle size distribution for the layers and Figure 15(b) shows the bulk density analysis for the layers. [3]

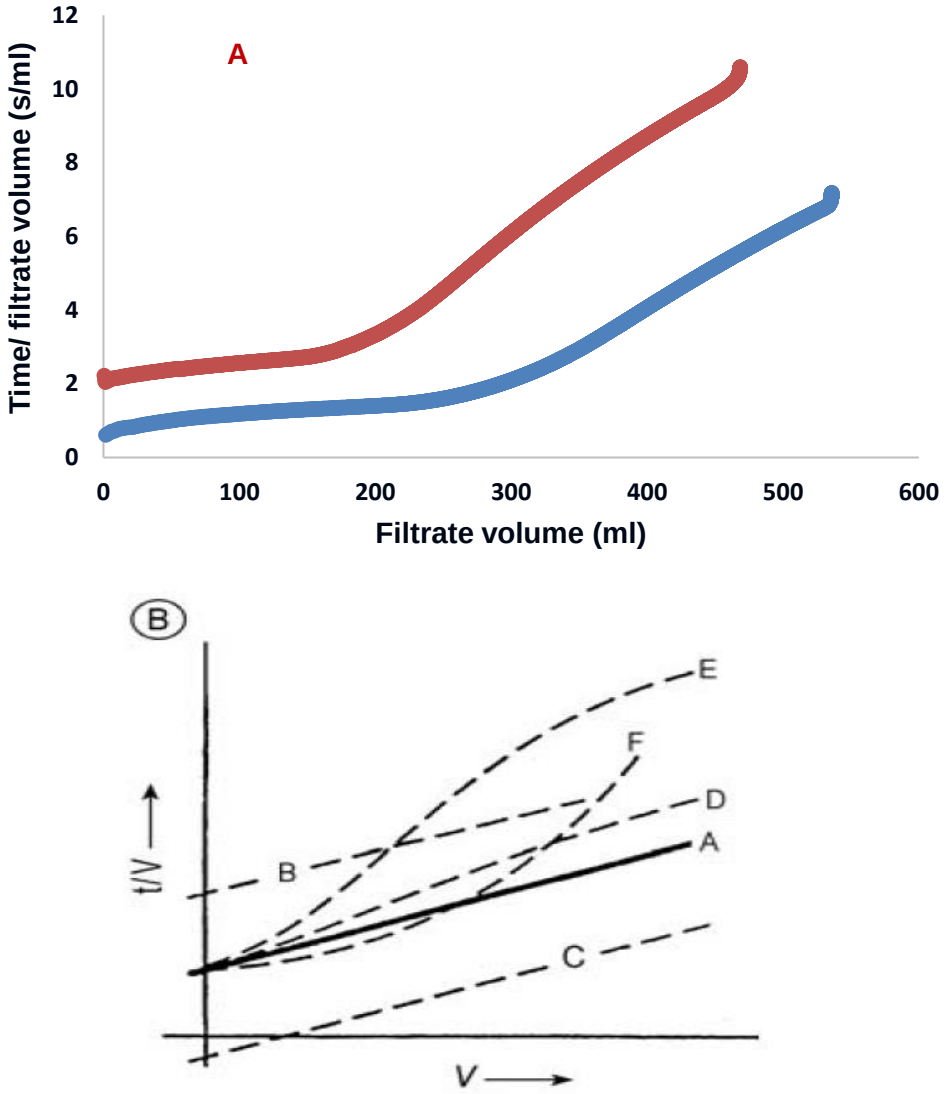

Figure 14: A. Plots of t/V vs. V for 900 mL slurry of 20% Catapal A surrogate and 1 micrometer screen mesh size within 25psi applied pressure drop B. integral plot for typical deviation from linearity [3]

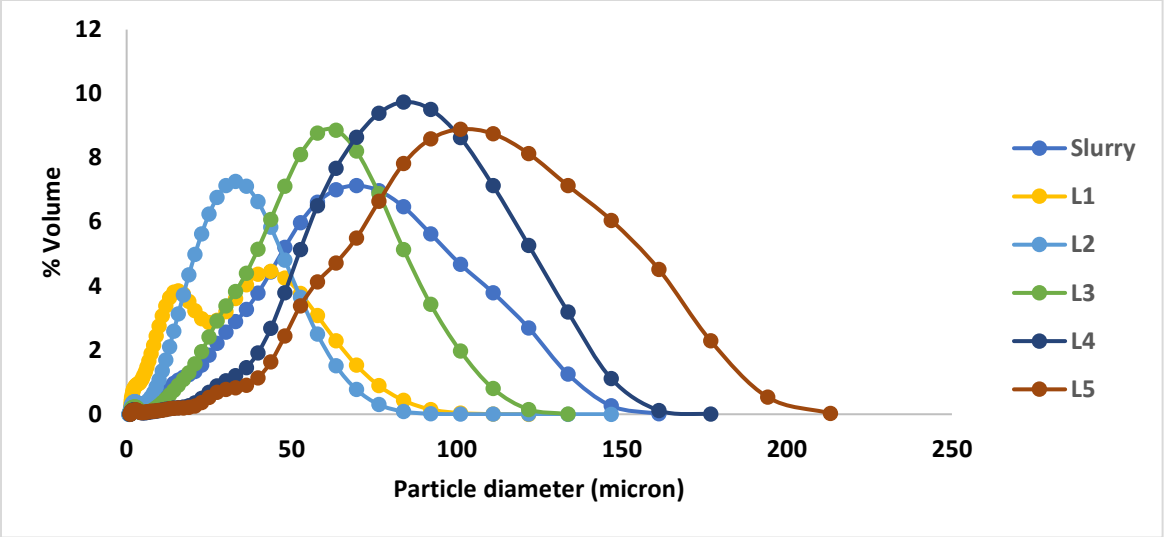

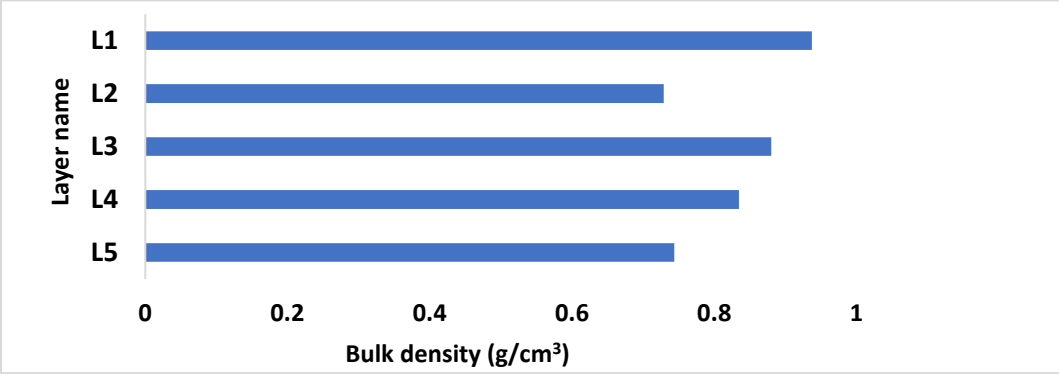

Figure 15: (a) Particle size distribution for the layers of the cake show that the average particle size increases as we go down to the base of the cake and is consistent for the last layers. (b) Bulk Density measurement of the layers of the cake

To mitigate the issue of settling, the particles were sieved with a 53 micron mesh. After sieving, the distribution becomes much narrower in comparison. The d50 of the particles reduced to 28.7 µm. The sieved and unsieved particle size comparisons can be seen in Figure 5. The fines of the sieved fraction are referred to as Fine Catapal A and the Unsieved Catapal A is referred to as Raw Catapal A.

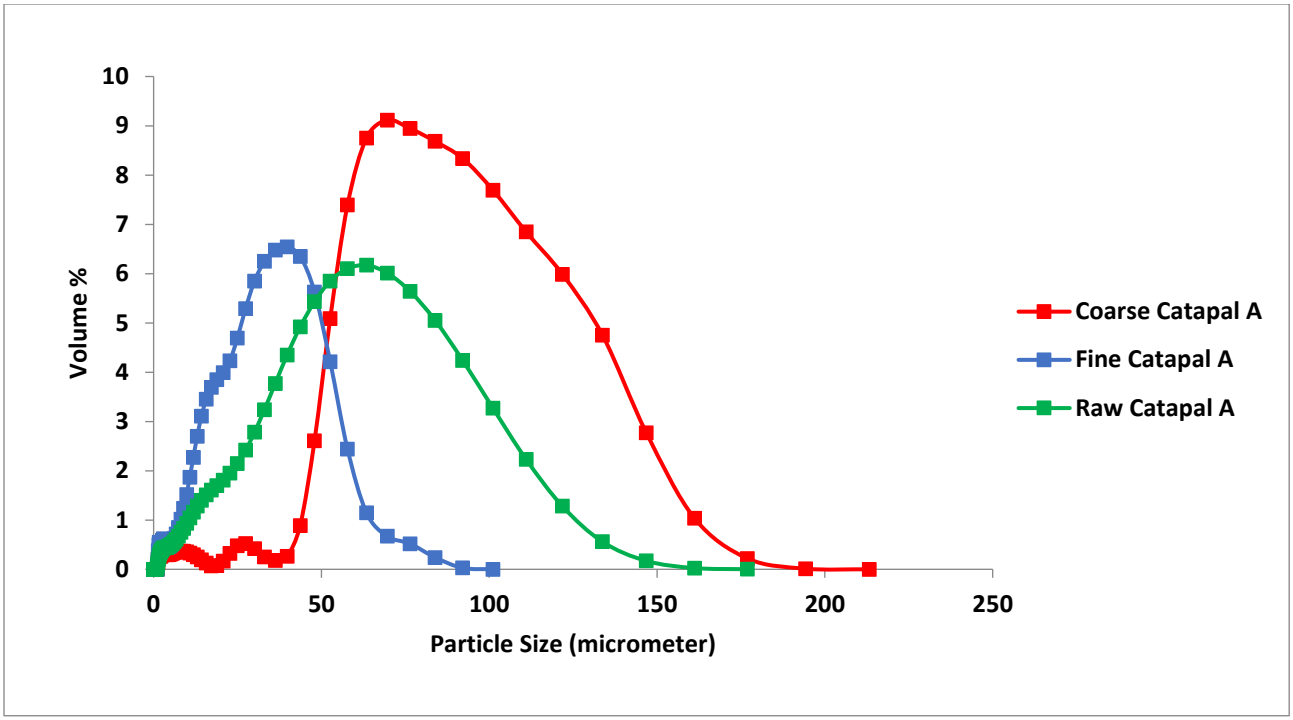

Figure 16: Comparison of Coarse, Fine and Raw Catapal A Particle size distributions measured by Laser Diffraction. The sieved particles have a narrower distribution.

Another change to mitigate settling is the reduction of slurry concentration from 20% w/w to 10% w/w as much more realistic parameter to simulate industry conditions.

The sieved particles were used in experimental filtration runs at three different pressures. All the runs were conducted at 10% solid concentration, 1 micron screen, 900mL slurry volume with varying pressure. The average permeabilities and cake resistances are depicted in Table 3.

Figure 17 shows the t/V vs V curves for each pressure.

Applied pressure (psi)	Permeability of cake x 10^{10} (cm^2)	Resistance of cake x 10^{-9} (cm^{-1})	Time of Filtration (minutes)
12	17 ± 1	0.77 ± 0.03	1.8±0.1
25	1.6 ± 0.8	11.0 ± 4.6	8.2±1
35	1.24	9.6	8.3

Table 3: Permeability of cake and Resistance of cake values for each pressure with 1 micron screen. The cake permeability is higher by an order of magnitude for 12 psi and for 25 psi and 35 psi the permeability and resistance are more consistent.

The values of permeability for 25psi and 35psi are on the same order of magnitude as that of glass beads. At 12 psi the permeability is significantly higher (one order of magnitude).

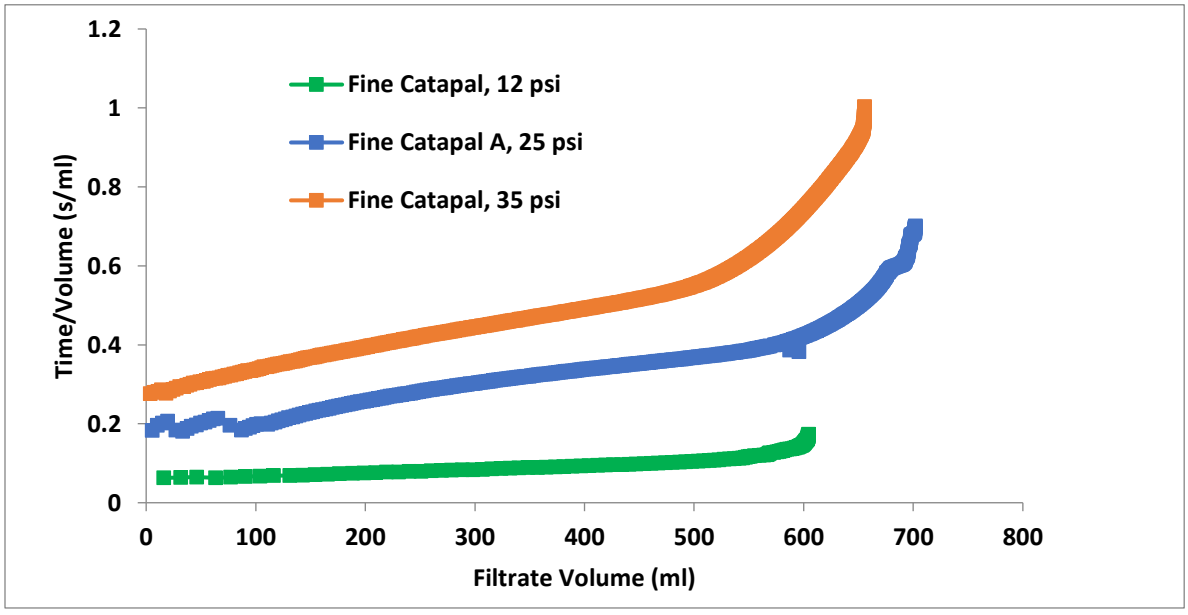

Figure 17: Plots of t/V vs. V for 900 mL slurry of 10% Fine Catapal A and 1 micrometer screen mesh size within 12 psi, 25 psi and 35 psi applied pressure drop.

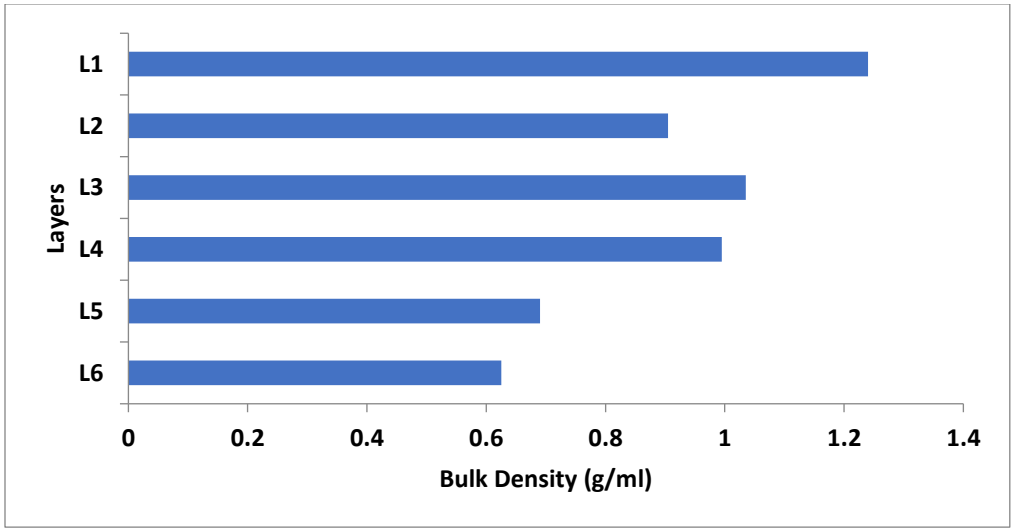

Figure 18: Bulk Density Layer Analysis for Filter Cake of Fine Catapal A, filtered at 12 psi with a 1 micron screen.

Analysis of the cake shows a trend of decreasing bulk density when moving from the top of the cake to the bottom-most layer. This indicates a higher percentage of fines in the upper layers. Analysis of the particle size distribution of the layers also shows that settling occurs.

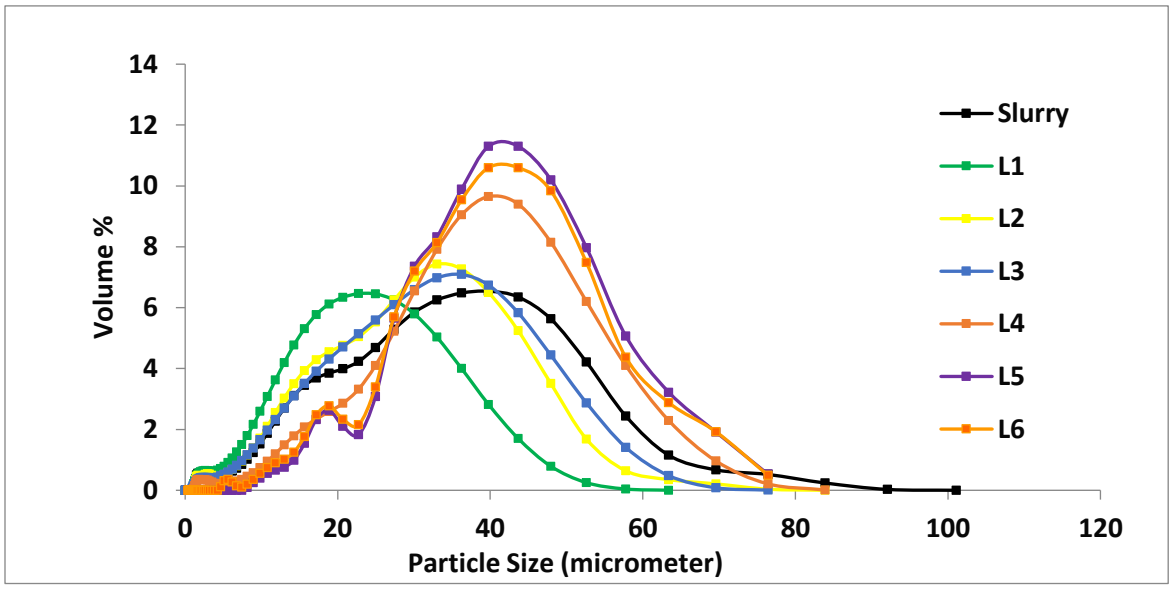

Figure 19: Particle Size Layer Analysis for Filter Cake of Fine Catapal A, filtered at 12 psi with a 1 micron screen.

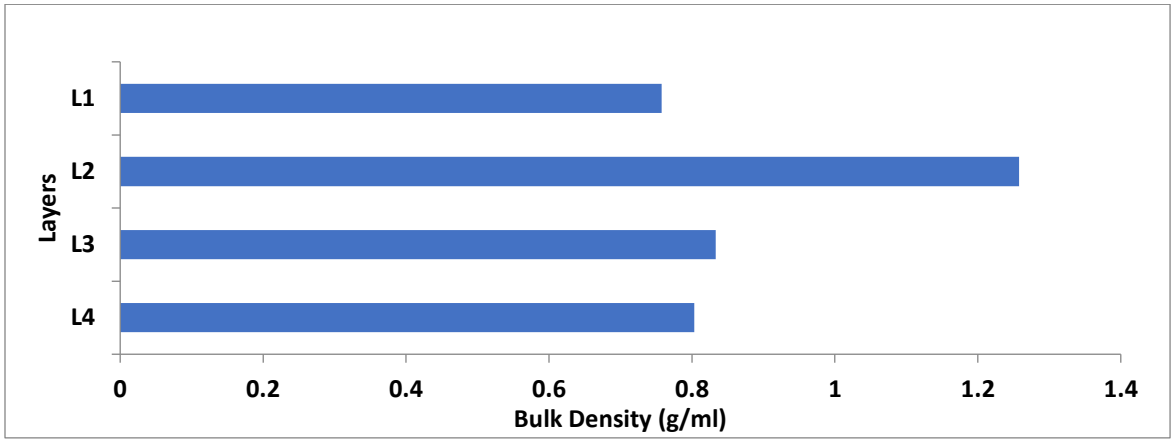

Figure 20: Bulk Density Layer Analysis for Filter Cake of Fine Catapal A, filtered at 25 psi with a 1 micron screen.

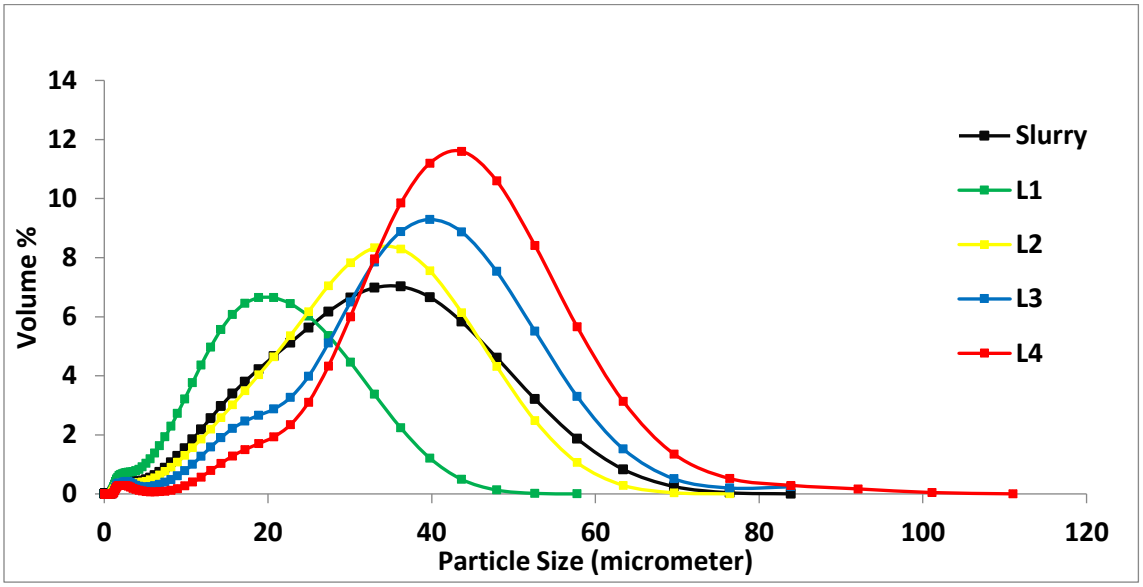

Figure 21: Particle size distribution Layer Analysis for Filter Cake of Fine Catapal A, filtered at 25 psi with a 1 micron screen.

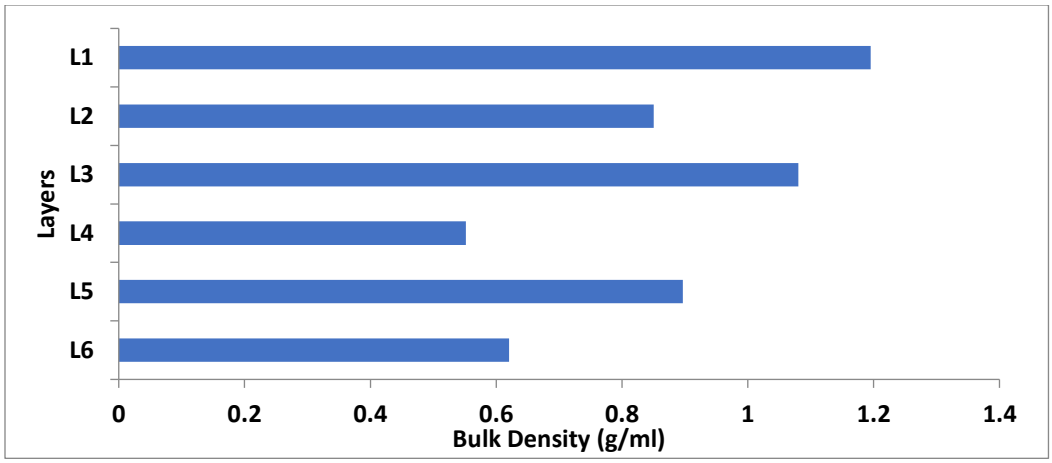

Figure 22: Bulk Density Layer Analysis for Filter Cake of Fine Catapal A, filtered at 35 psi with a 1 micron screen.

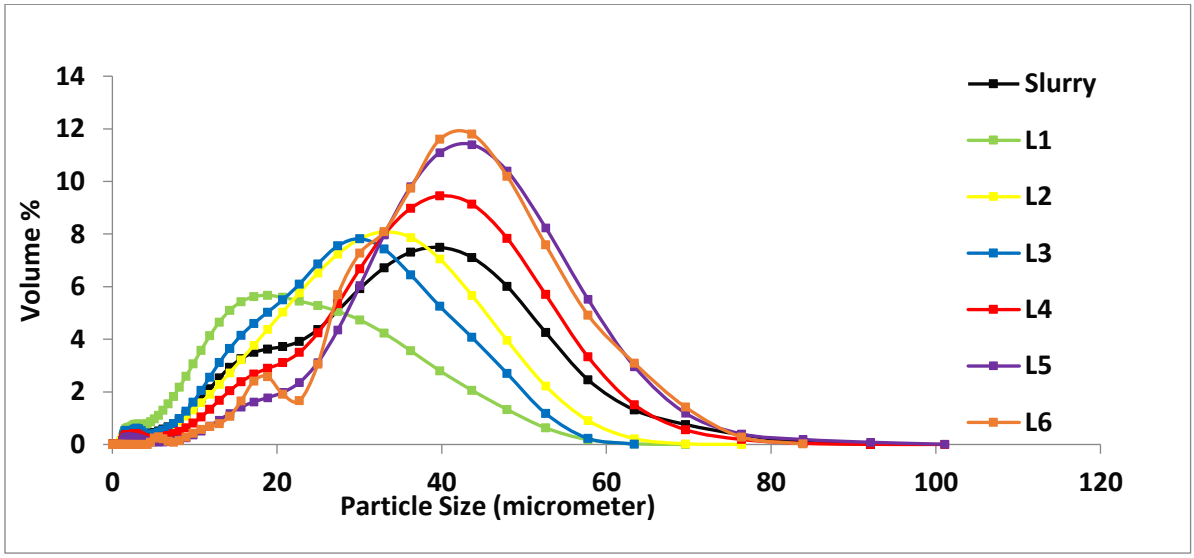

Figure 23: Particle size distribution Layer Analysis for Filter Cake of Fine Catapal A, filtered at 35 psi with a 1 micron screen.

	Fines/Coarse		
Layer	12 psi	25 psi	35 psi
Slurry	0.29	0.25	0.25
L1	1.13	1.19	1.03
L2	0.40	0.23	0.35
L3	0.36	0.10	0.49
L4	0.14	0.05	0.16
L5	0.08		0.08
L6	0.10		0.08

Table 4: Fines/Coarse ratio for each layer in the Fine Catapal A cake at 12 psi, 25 psi and 35 psi

Fine Alumina was run at 12psi and 35psi, at 10% w/w concentration with a volume of 900ml. The values of the permeability and resistance are given below in *Table 5*.

Applied pressure (psi)	Permeability of cake x 10^{10} (cm^2)	Resistance of cake x 10^{-9} (cm^{-1})	Height of Cake (cm)	Time of filtration (minutes)
12 psi	0.59±0.02	41.5±0.7	2.4	33.6±1.4
35 psi	0.66±0.05	34.5±0.2	2.4	10.8±0.3

Table 5: Permeability and cake resistance values for Fine Alumina at two different pressures, 12 psi and 35 psi.

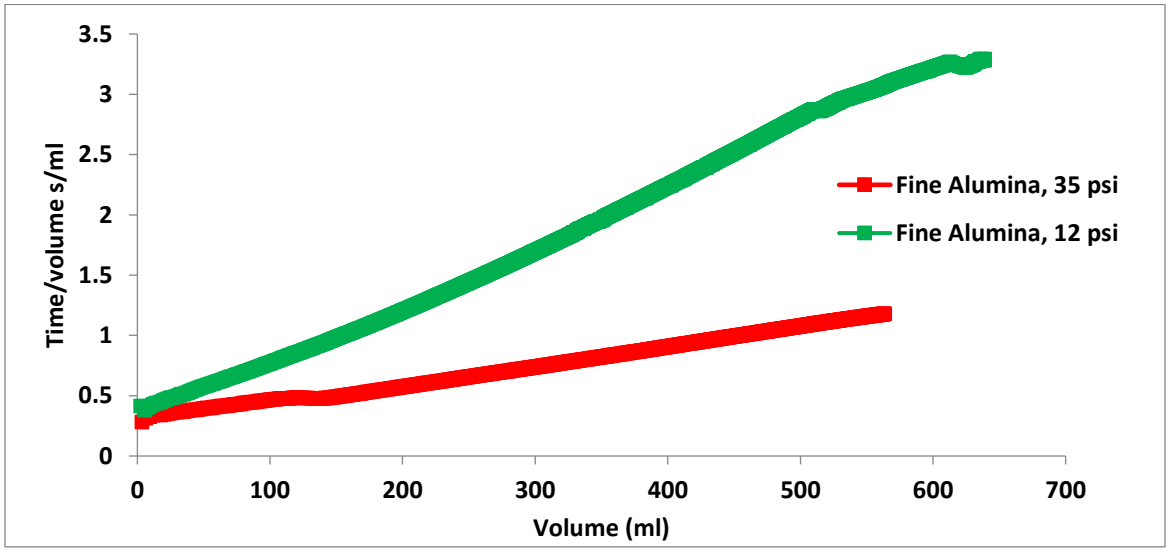

Figure 24: Time/Volume vs Volume for Fine Alumina at 12 psi, 35 psi with 1 micron screen

The Figure above is the plot of Time/Volume vs Volume for Fine Alumina filtered through a 1 micron screen at 12psi and 35 psi. The Fine Alumina filtered much faster at 35 psi, however the resistance and permeability of the cake are of the same order of magnitude.

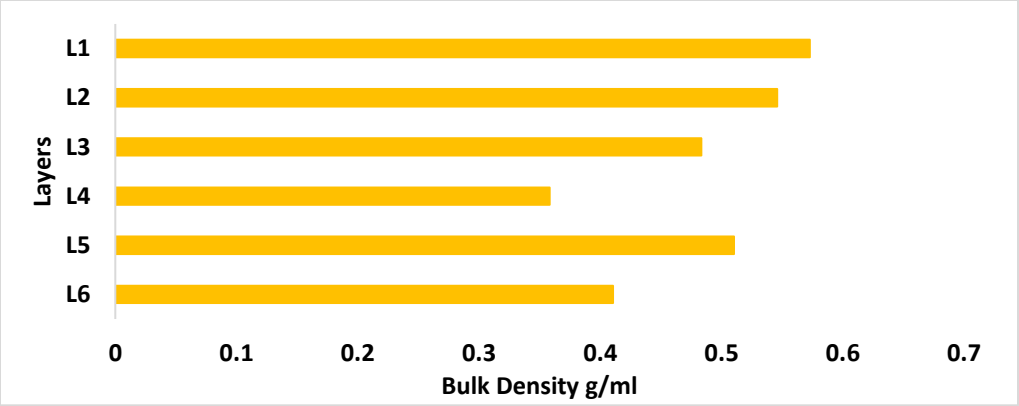

Figure 25: Bulk Density Layer Analysis for Filter Cake of Fine Alumina, filtered at 35 psi with a 1 micron screen.

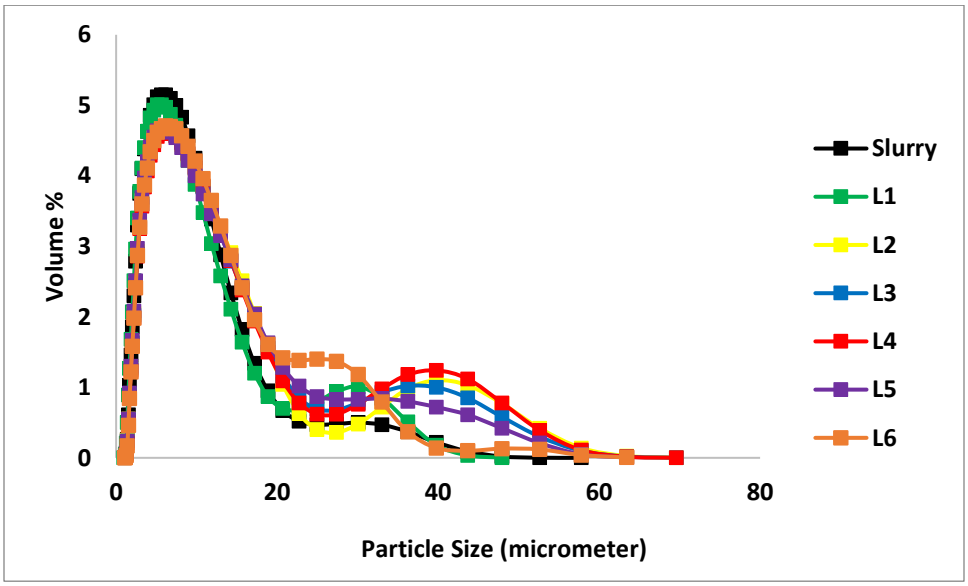

Figure 26: Particle size distribution Layer Analysis for Filter Cake of Fine Alumina, filtered at 35 psi with a 1 micron screen.

Comparing the Bulk Densities of each layer of Fine Catapal A and Fine Alumina by normalizing it with the average Bulk Density to see the differences between Fine Catapal A, Fine Alumina. It easy to see that in comparison to Fine Alumina, the Fine Catapal A is more separated i.e. more settling.

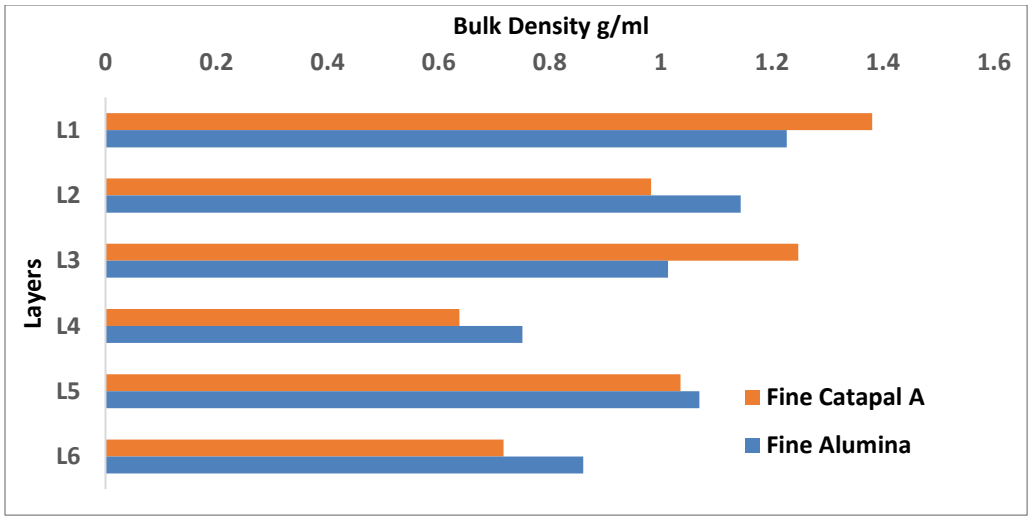

Figure 27: Normalized Bulk Density comparison between Fine Catapal A and Fine Alumina for filter cakes from 35 psi runs with a 1 micron screen.

Zeolite Y was run at 12 psi, 10% w/w concentration with a volume of 900ml. The slurry was easy to suspend and did not settle within the time it was poured into the reactor. On plotting t/v vs V, permeability to the order of 10^{-11} is observed. The values can be seen in the table below in comparison to Fine Catapal A and Fine Alumina at the same pressure. Zeolite Y has a higher cake resistance and lower permeability than both Fine Alumina and Fine Catapal A. It also took a long time to filter (more than ten times higher than Fine Catapal A).

	Permeability of cake x 10^{10} (cm^2)	Resistance of cake x 10^{-9} (cm^{-1})	Height of Cake (cm)	Time of filtration (minutes)
Fine Catapal A	17 ± 1	0.8 ± 0.03	1.3	1.8±0.1
Fine Alumina (FA)	0.59±0.02	41.5±0.7	2.4	33.6±1.4
Zeolite Y	0.23	61.7	1.4	52.3

Table 6: Permeability and cake resistance values for Fine Catapal A, Fine Alumina and Zeolite Y at 12psi.

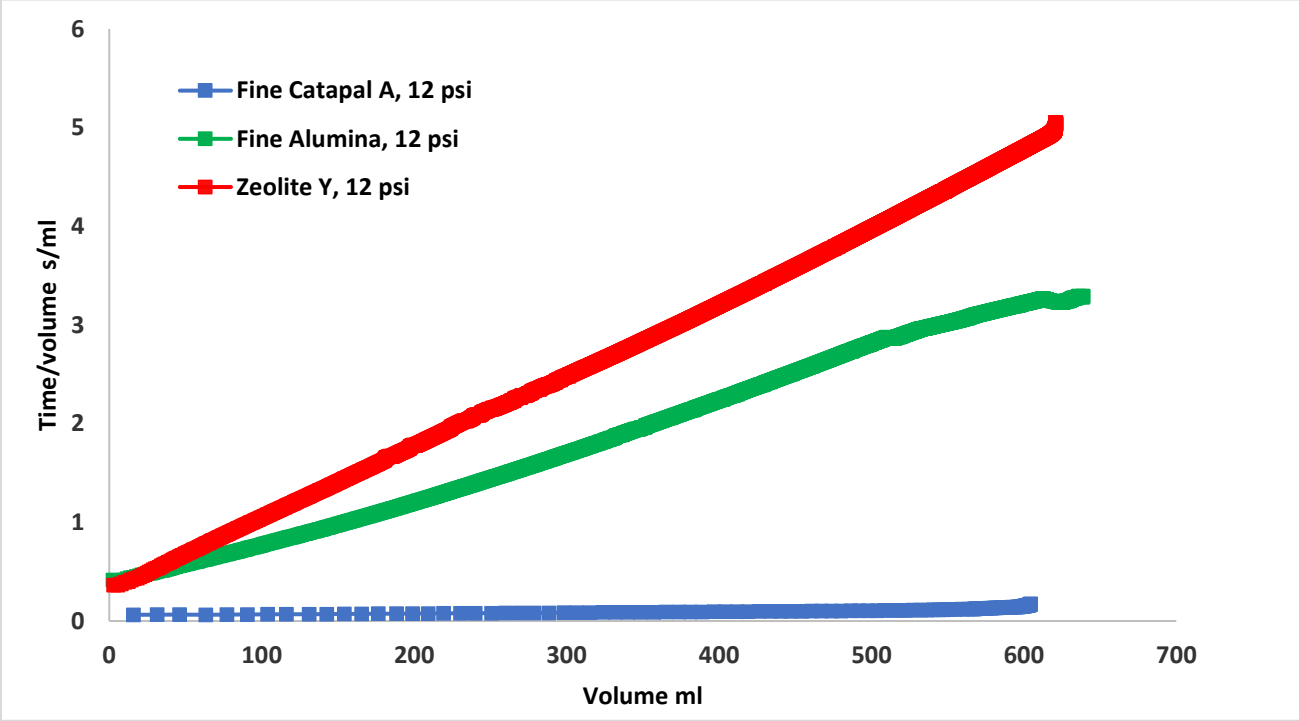

Figure 28: Time/Volume vs Volume for Fine Catapal A, Fine Alumina and Zeolite Y at 12 psi

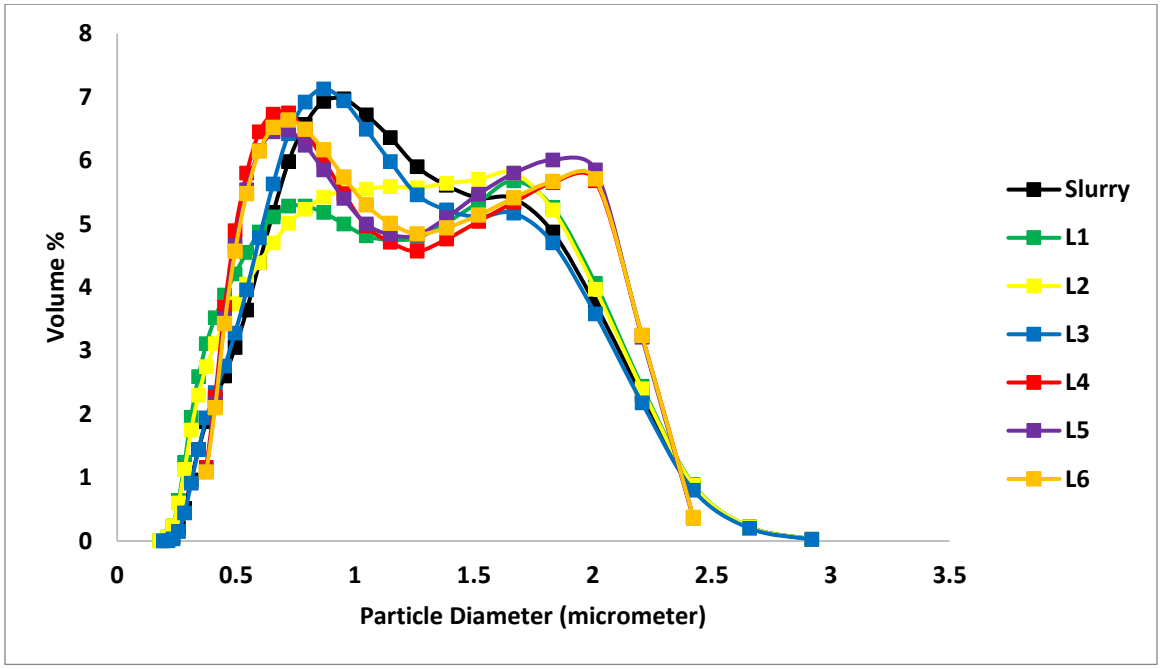

Figure 29: Particle size distribution Layer Analysis for Filter Cake of Zeolite Y, filtered at 12 psi with a 1 micron screen.

viii. Batch Filtration of Coarse and Fine Mixture

Experiments were run on slurries with a percentage of fines to see the effect on fines on the permeability of the filter cake. A mixture was made with Fine Alumina and Coarse Alumina (i.e. Fine Catapal A).

The mixtures were run at 10% total solid concentration, of which 1.1% is fine alumina and 8.9% is coarse alumina. The mixture was run at 12 psi and 900mL slurry volume filtered with a 1-micron screen.

The particle size distribution of the pure components measured by laser diffraction is displayed in *Figure 30*.

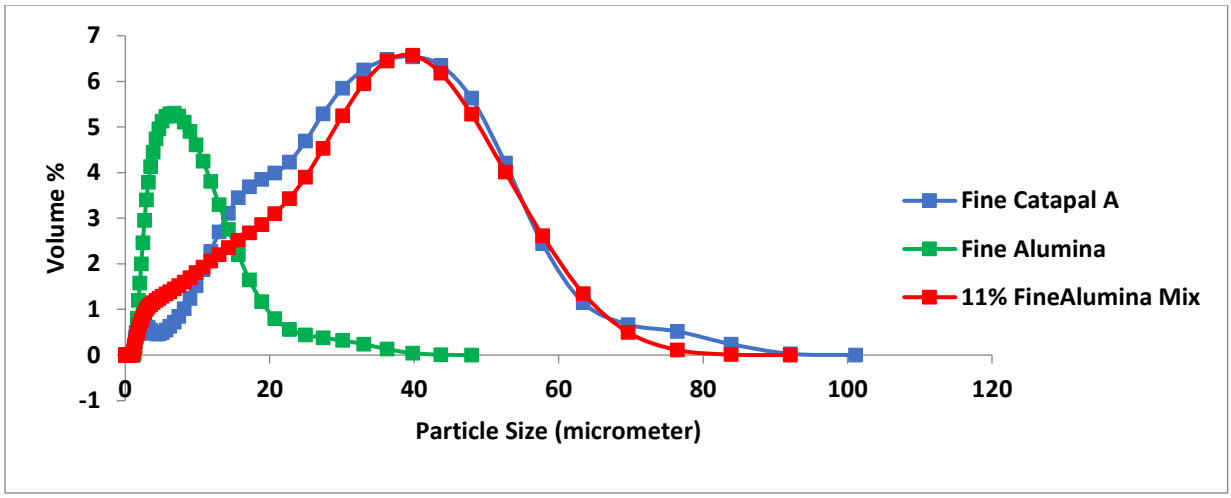

Figure 30: Comparison of Fine Catapal A, Fine Alumina and 11% Fine Alumina and 89% Coarse Alumina (*Fine Catapal A*) *slurry in water*

To calculate permeability, t/V vs V was plotted for each run and the permeability and the resistance of the cake were calculated from the slope and intercept of the curve. The graphs are displayed in *Figure 31*. The permeability and intercept values are displayed in *Table 7.* Pure Fine Alumina has a much lower permeability than that of Coarse Alumina at 12 psi. The results show that at 12 psi, a small percentage of fines (11% of total solids) can alter the permeability significantly and reduce the permeability of the cake to that of pure Fine Alumina.

The fine increase can be seen as a slight “bump” in the 0-20 µm range. As can be seen in Table 7, the time of Filtration greatly increases with just the addition of 11% fines.

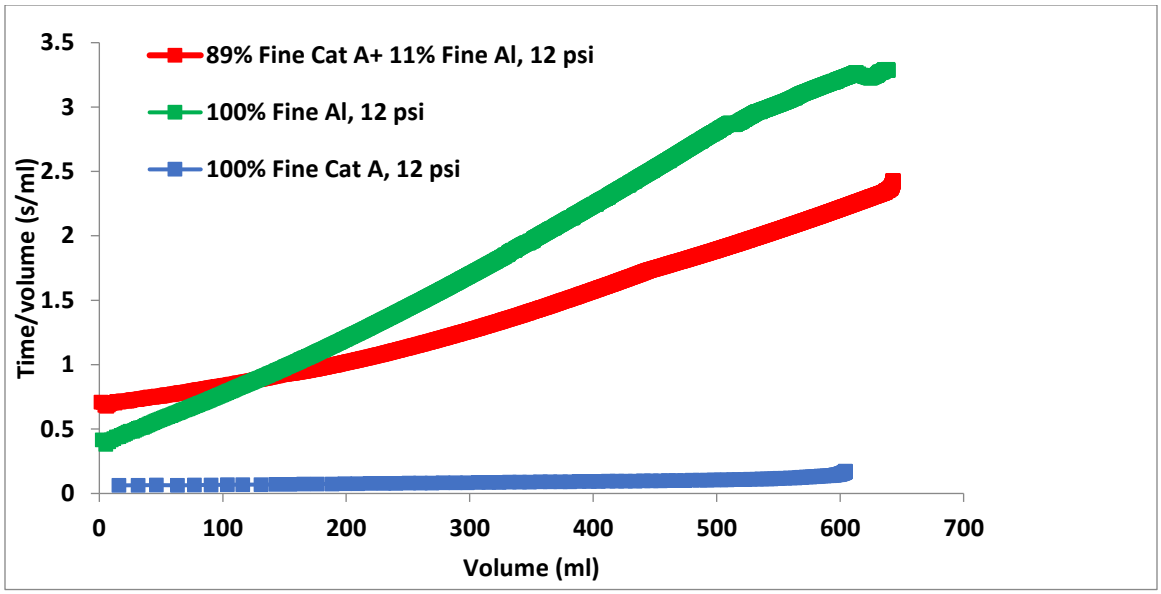

Figure 31: Plots of t/V vs. V for 900 mL slurry of 10% Fine Catapal A, 10% Fine Alumina and 1.1% FA and 8.9% CA and 1 micrometer screen mesh size at 12 psi applied pressure drop.

	Permeability of cake x 10^{10} (cm^2)	Resistance of cake x 10^{-9} (cm^{-1})	Height of Cake (cm)	Time of filtration (minutes)
Fine Catapal A (FCA)	17 ± 1	0.77 ± 0.03	1.3	1.8±0.1
Fine Alumina (FA)	0.59±0.02	41.5±0.7	2.4	33.6±1.4
11% FA + 89% FCA	0.56 ± 0.01	25.1 ± 0.6	1.4	25.3±0.7

Table 7: Permeability of cake and Resistance of cake values for each material at 12 psi with 1 micron screen. Experimental values of Cake height and Time of Filtration are also depicted.

ix. Continuous Filtration of Porous Particles

The filtration runs with the continuous filter did not give results showing a similar trend, as expected. The advantage of having a continuously mixing system is that there is no limitation due to settling of larger particles. Therefore, runs could be conducted with particles of a much larger mean particle size and the results would not be influenced by settling. Runs were conducted on Coarse Catapal A and Raw Catapal A along with Fine Catapal A and Fine Alumina.

	Resistance of cake x 10^{-9} (cm^{-1})	Time of filtration for 200mL (minutes)
Fine Catapal A (FCA)	60.6	1.6
Coarse Catapal A (CCA)	342	62.1
Fine Alumina (FA)	52.2	8.2
8.9% FCA + 1.1% FA	59.2	10.25

Table 8: Cake resistance and Time of Filtration for 200mL for Continuous filtration runs conducted at 35 psi and 1 micron screen.

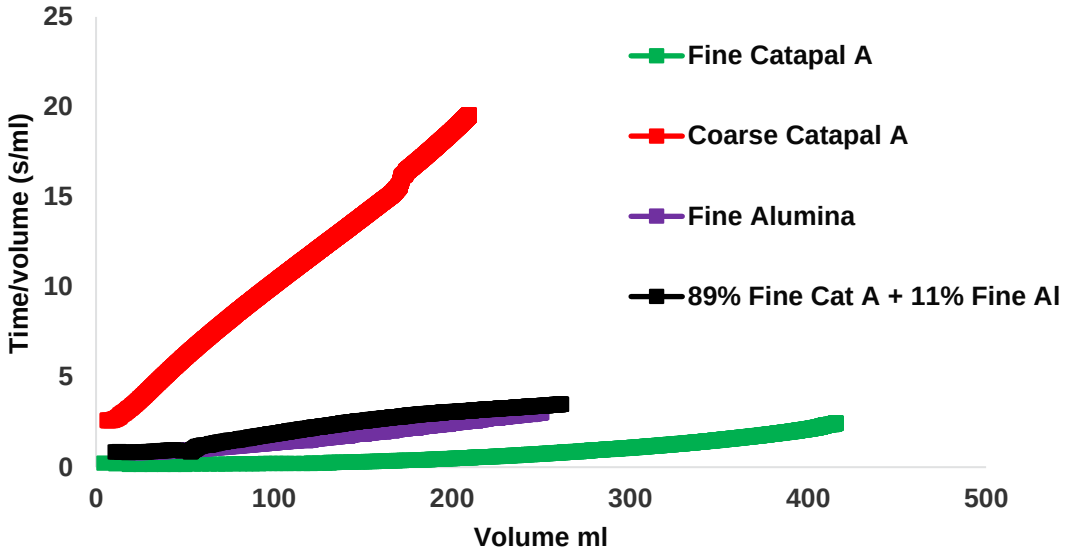

Figure 32: Filtration curves of t/v vs V for continuous filtration at 35 psi and 1 micron screen.

Comparing results from the continuous system, Fine Alumina and 11% Fine Alumina display similar filtration behavior to each other, with similar cake resistances and similar filtration time for 200ml. They also display a higher resistance than Fine Catapal A, which is similar to what is observed in the batch filter at Rutgers. The filtration behavior of Coarse Catapal A is unexpected. The cake resistance is much higher than is expected for permeability to scale with the median diameter squared of a monodisperse slurry. However, these aren't monodisperse powders. The wide particle size distribution and the lack of settling to cause layer separation increases the cake resistance. The fines in the slurry plug the interparticle pores and dramatically increase cake resistance. The PSD is plotted in *Figure 33* below.

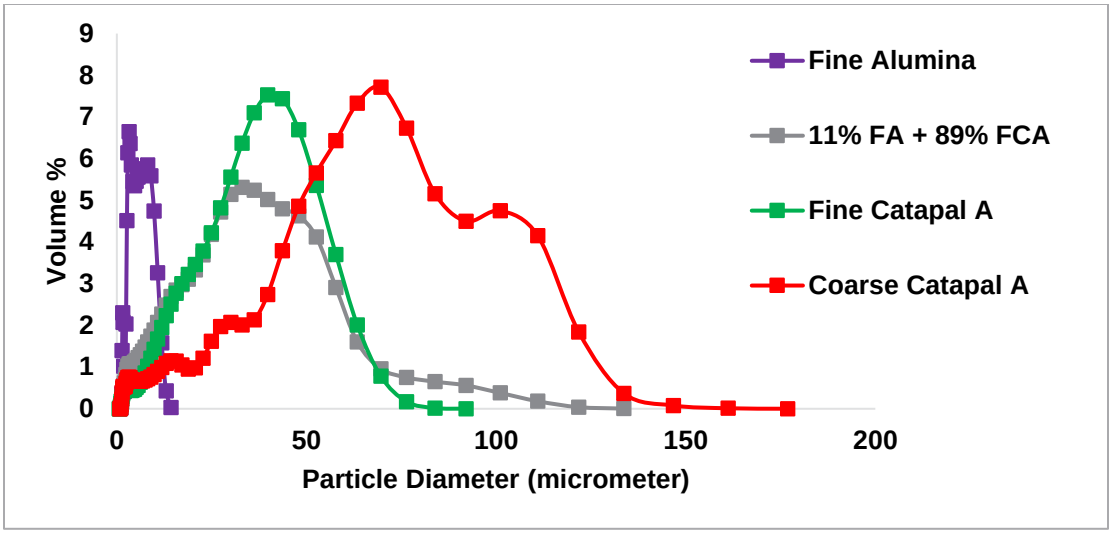

Figure 33: Particle size distribution of slurries sampled from the reactor that feeds into filter housing for runs with Fine Alumina, Fine Catapal , Coarse Catapal A, Fine Alumina and Fine Catapal A mixture at 35 psi.

These results lead to the conclusion that the breadth of the particle size distribution is a major influencer of filtration behavior.

Directly comparing batch and continuous filtration, at 12psi we can see that for every batch run, the continuous run shows a higher cake resistance and a longer run for 200mL of filtrate. It is also apparent that differences in cake resistance and run time are much less pronounced for Fine Alumina than for Fine Catapal A, presumably due to the smaller extent of settling experienced by Fine Alumina in the Rutgers filter, as confirmed by cake analysis. Finally, differences in cake resistance and run time are much less pronounced for both materials at 35 psi compared to 12 psi applied pressure. This result suggests that the higher applied pressure also works against settling by generally reducing the time of the experiment and possibly forces particles into a more open or disordered structure than that formed at lower pressure.

Referring back to methodology, efforts were made to recreate a similar procedure that had been done for batch runs, so that the only major difference is the lack of large particles settling close to the screen.

That leads to the conclusion that the settling helps create a cake that has a lower resistance for easier filtering. Results given in **RED** are Batch Filtration and those in **BLUE** are Continuous filtration.

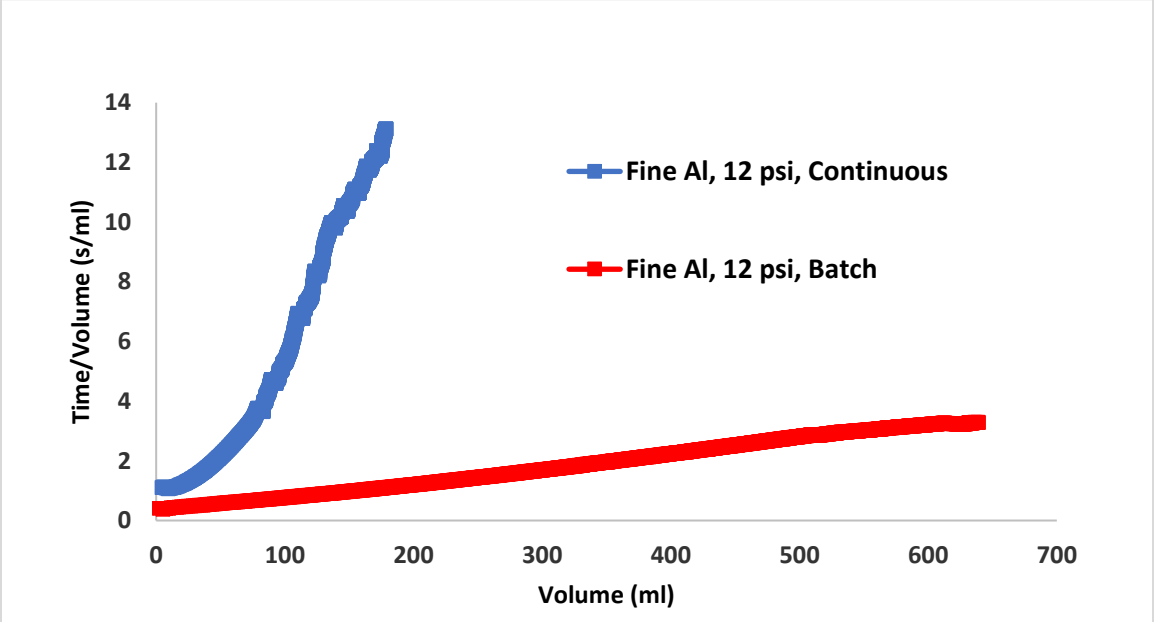

Figure 34: Fine Alumina Filtration run curves at 12 psi and 1 micron screen.

Fine Alumina at 12 psi	
Time for 200 mL (minutes)	Resistance of cake x 10-9 (cm^{-1})
5.4±1.5	41.5±0.7
39+	103

Table 9: Fine Alumina Filtration results for cake resistance and time of filtration for 200mL at 12 psi. Results given in RED are Batch Filtration and those in BLUE are Continuous filtration.

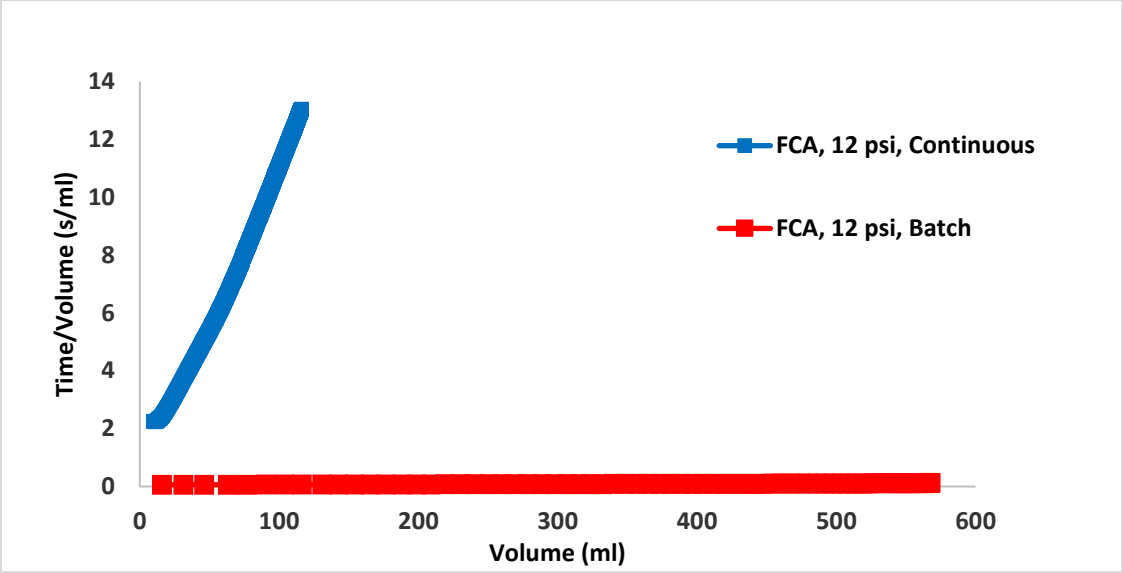

Figure 35: Fine Catapal A Filtration run curves at 12 psi and 1 micron screen.

Fine Catapal A at 12 psi	
Time for 200 mL (minutes)	Resistance of cake x 10-9 (cm^{-1})
0.25	0.77±0.08
37.9	94.7

Table 10: Fine Catapal A Filtration results for cake resistance and time of filtration for 200mL at 12 psi. Results given in RED are Batch Filtration and those in BLUE are Continuous filtration.

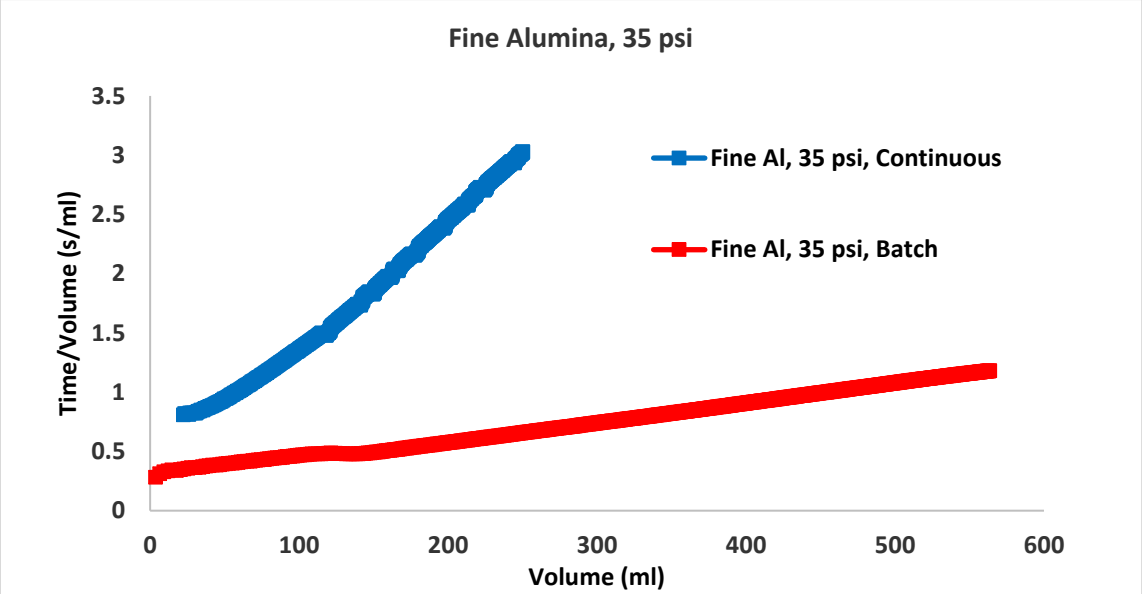

Figure 36: Fine Alumina Filtration run curves at 35 psi

Fine Alumina at 35 psi	
Time for 200 mL (minutes)	Resistance of cake x 10-9 (cm^{-1})
2.6±0.7	36.3±0.2
8.2	52.2

Table 11: Fine Alumina Filtration results for cake resistance and time of filtration for 200mL at 35 psi and 1 micron screen. Results given in RED are Batch Filtration and those in BLUE are Continuous filtration.

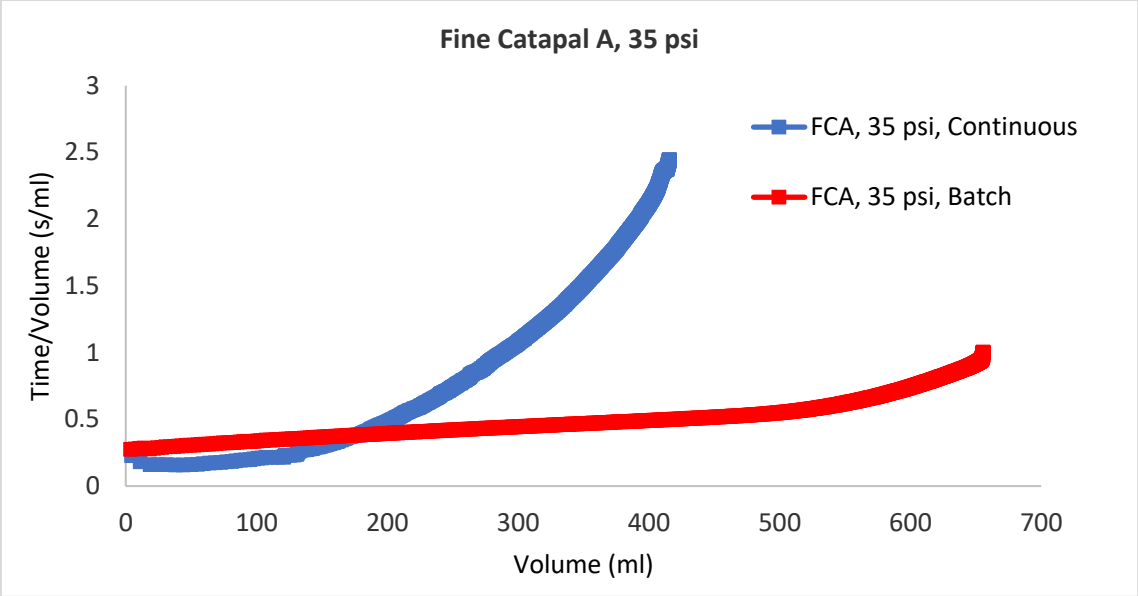

Figure 37: Fine Catapal A Filtration run curves at 35 psi and 1 micron screen.

Fine Catapal A at 35 psi	
Time for 200 mL (minute)	Resistance of cake x 10-9 (cm^{-1})
1.3	9.65
1.6	60.6

Table 12: Fine Catapal A Filtration results for cake resistance and time of filtration for 200mL at 12 psi. Results given in RED are Batch Filtration and those in BLUE are Continuous filtration.

V. CONCLUSION

The benchtop Nutsche filter was used to run constant pressure filtration experiments on porous particles to observe filterability. The materials were incompressible in aqueous slurry form and the permeability did not have a strong dependence on pressure.

Based on the results it can be concluded that for the 1 litre batch system the dominating mechanism is settling. If the particles are large enough, they settle, forming an initial loosely packed structure making the overall cake more permeable.

For a broad size distribution the initial layer separation with the bottom-most layers being coarse results in an in-situ filter aid and easier filtration (lower cake resistance and higher cake permeability).

Analyzing normalized bulk density for each layer of the filter cake for both fine alumina and Fine Catapal A shows a greater extent of layer separation for Fine Catapal A.

The filtration run was also dominated by the percentage of fines. Experiments on mixtures of Fine Alumina and Fine Catapal A show that a small percentage of fines can dominate the filtration run leading to filtration times closer to that of Fine Alumina than Fine Catapal A.

Running filtration experiments in a continuous setting and comparing the cake resistances to those measured in a batch system, it can be seen that when settling isn't the dominating mechanism, the results change drastically. The permeability doesn't scale with the median particle size and with no layer separation and in-situ filter aid formation, the wider distribution is still dominated by the fines.

Continuous filtration has cake resistances are at least an order of magnitude higher than their equivalent batch runs. This makes clear the value of layer separation, an in-situ filter aid would reduce the time of filterability and allowing for layer separation would require very minimal pre treatment before filtration. Depending on the equipment, this could be as easy as allowing a waiting time before pressure is applied.

VI. REFERENCES

1. Wakeman, R., *The influence of particle properties on filtration.* Separation and Purification Technology, 2007. **58**(2): p. 234-241.
2. Richardson, J.F., J.H. Harker, and J.R. Backhurst, *CHAPTER 4 - Flow of Fluids through Granular Beds and Packed Columns*, in *Chemical Engineering (Fifth Edition)*, J.F. Richardson, J.H. Harker, and J.R. Backhurst, Editors. 2002, Butterworth-Heinemann: Oxford. p. 191-236.
3. Riperger, S., *Ullmann's Encyclopedia of Industrial Chemistry*. 2003: John Wiley & Sons.
4. Basim, G.B. and M. Khalili, *Particle size analysis on wide size distribution powders; effect of sampling and characterization technique.* Advanced Powder Technology, 2015. **26**(1): p. 200-207.
5. Kinnarinen, T., R. Tuunila, and A. Häkkinen, *Reduction of the width of particle size distribution to improve pressure filtration properties of slurries.* Minerals Engineering, 2017. **102**: p. 68-74.
6. M. Bricker, J., *Oscillatory shear of suspensions of noncolloidal particles*. Vol. 50. 2006.
7. Iritani, E., *Properties of Filter Cake in Cake Filtration and Membrane Filtration.* KONA Powder and Particle Journal, 2003. **21**: p. 19-39.
8. Alam, N., et al., *Dewatering of coal plant tailings: Flocculation followed by filtration.* Fuel, 2011. **90**(1): p. 26-35.
9. Kinnarinen, T., et al., *Recovery of sodium from bauxite residue by pressure filtration and cake washing.* International Journal of Mineral Processing, 2015. **141**: p. 20-26.
10. Pearlmutter, B.A., *Selection of Filters for the Separation Process.* Chemical Engineering World, Dec. 2009: p. 68-74.
11. Raymond Bonne, E.S., *Filtration and Washing of Catalysts,*.
12. Barry A. Perlmutter, P.M.D.-B.-F.I., *A REVIEW OF FILTER PRESS BASICS AND ISSUES VERSUS ALTERNATIVE BATCH OR CONTINUOUS REPLACEMENT TECHNOLOGIES*
13. Nittami, T., et al., *Effect of compressibility of synthetic fibers as conditioning materials on dewatering of activated sludge.* Chemical Engineering Journal, 2015. **268**: p. 86-91.
14. Ruth, B.F., G.H. Montillon, and R.E. Montonna, *Studies in Filtration - I. Critical Analysis of Filtration Theory.* Industrial & Engineering Chemistry, 1933. **25**(1): p. 76-82.
15. Ruth, B.F., *Studies in Filtration. II. Fundamental Axiom of Constant-Pressure Filtration.* Ind. Eng. Chem., 1933. **25**: p. 153-161.
16. Inam, M.A., S. Ouattara, and C. Frances, *Effects of concentration of dispersions on particle sizing during production of fine particles in wet grinding process.* Powder Technology, 2011. **208**(2): p. 329-336.
17. Koltermann, C.E. and S.M. Gorelick, *Fractional packing model for hydraulic conductivity derived from sediment mixtures.* Water Resources Research, 1995. **31**(12): p. 3283-3297.
18. Teoh, S.-K., R.B.H. Tan, and C. Tien, *Analysis of cake filtration data—A critical assessment of conventional filtration theory.* AIChE Journal, 2006. **52**(10): p. 3427-3442.
19. Ripperger, S., et al., *Ullmann's Encyclopedia of Industrial Chemistry: Filtration, 1. Fundamentals*. 1-38.
20. Holland, F.A. and R. Bragg, *9 - Fluid motion in the presence of solid particles*, in *Fluid Flow for Chemical Engineers (Second Edition)*, F.A. Holland and R. Bragg, Editors. 1995, Butterworth-Heinemann: Oxford. p. 288-304.
21. Hieke, M., et al., *Analysis of the Porosity of Filter Cakes Obtained by Filtration of Colloidal Suspensions.* Chemical Engineering & Technology, 2009. **32**(7): p. 1095-1101.

22. Tien, C. and B.V. Ramarao, *Can filter cake porosity be estimated based on the Kozeny–Carman equation?* Powder Technology, 2013. **237**: p. 233-240.
23. Scicolone, J.V., et al., *Effect of liquid addition on the bulk and flow properties of fine and coarse glass beads.* AIChE Journal, 2016. **62**(3): p. 648-658.
24. Glasser, B.J., *Pharmaceutical Process Design I: Synthesis, Separations, and Sterile Processing.* Lecture notes on Pharmaceutical filtration processes, 2014.
25. Rheometer, A.t.F.P., *Compressibility.* www.freemantech.co.uk.
26. Rheometer, A.t.F.P., *Permeability.* www.freemantech.co.uk.
27. Barry A. Perlmutter, P.M.D.-B.-F.I., *COMBINATION FILTRATION OF PRESSURE, VACUUM AND CLARIFICATION TECHNOLOGIES FOR OPTIMUM PROCESS SOLUTIONS*
28. Ripperger, S., et al., *Filtration, 2. Equipment. In Ullmann's Encyclopedia of Industrial Chemistry,*. 2013.